Doctor of Philosophy

Vorinostat promotes with melatonin the therapeutic sensitivity in glioblastoma and glioma stem cells

The Graduate School
Of The University of Ulsan

Department of Medicine
Gi-Jun Sung

Vorinostat promotes with melatonin the therapeutic sensitivity in glioblastoma and glioma stem cells

Supervisor : Kyung-Chul Choi

A Dissertation

Submitted to
The Graduate School of the University of Ulsan
In partial Fulfillment of the Requirements
For the Degree of

Doctor of Philosophy

by

Gi-Jun Sung

Department of Medicine
Ulsan, Korea
August 2019

Vorinostat promotes with melatonin the therapeutic sensitivity in glioblastoma and glioma stem cells

This certifies that the dissertation of Gi-Jun Sung is approved

---

Committee Chair Dr. Jaekyoung Son

Committee Member Dr. Kyung-Chul Choi

Committee Member Dr. Sung-Hak Kim

Committee Member Dr. Yong Shin

Committee Member Dr. Chang Hoon HA

Department of Medicine

Ulsan, Korea

August 2019

Abstract

Glioblastoma (GBM) is the most aggressive malignant glioma and most lethal form of human brain cancer. GBM is also one of the most expensive and difficult cancers to treat by the surgical resection, local radiotherapy and temozolomide (TMZ) and still remains an incurable disease. Oncomine platform analysis and Gene Expression Profiling Interactive Analysis (GEPIA) show that the expression of transcription factor EB (TFEB) was significantly increased in GBMs and in GBM patients above stage IV. TFEB requires the oligomerization and localization to regulate transcription in the nucleus. Also, the expression and oligomerization of TFEB proteins contribute to the resistance of GBM cells to conventional chemotherapeutic agents such as TMZ. Thus, we investigated whether the combination of vorinostat and melatonin could overcome the effects of TFEB and induce apoptosis in GBM cells and glioma cancer stem cells (GSCs). The downregulation of TFEB and oligomerization by vorinostat and melatonin increased the expression of apoptosis-related genes and activated the apoptotic cell death process. Significantly, inhibition of TFEB expression dramatically decreased GSC tumor-sphere formation and size. The inhibitory effect of co-treatment resulted in decreased proliferation of GSCs, and induced the expression of cleaved-PARP and p-γH2AX. Taken together, our results definitely demonstrate that TFEB expression contributes to enhanced resistance of GBMs to chemotherapy and that vorinostat and melatonin activated apoptosis signaling in GBM cells by inhibiting TFEB expression and oligomerization, suggesting that co-treatment of vorinostat and melatonin may be an effective therapeutic strategy for human brain cancers.

Key words: TFEB, Oligomerization, Localization, Glioblastoma, Vorinostat, Melatonin

CONTENTS

LIST OF FIGURES

Introduction

Glioblastoma (GBM) is the most frequent and most lethal type of malignant human brain tumor[1]. Current treatment for GBM consists of chemotherapy with the oral alkylating agent temozolomide and the antiangiogenic agent bevacizumab, a humanized monoclonal antibody that binds to vascular endothelial growth factor (VEGF) with high affinity[2),3)]. Treatment failure is frequent, however, and is likely due to the survival of refractory cancer cells, which have the stemness properties of GBM-derived tumor spheres or glioma cancer stem cells (GSCs). Most GBMs are characterized by gene alterations, which affect the genes that control tumorigenicity via a process of epigenetic modification. Chromatin alterations due to histone modifications have also been associated with the molecular pathology of GBM. According to the Cancer Genome Atlas research network, GBM recurrence is directly linked to epigenetic mechanisms for histone remodeling. Because these epigenetic changes have been associated with the enzyme histone deacetylase (HDAC), HDAC inhibitors have been developed for clinical trials in patients with GBM[4),5)].

Preclinical studies have shown that HDAC inhibitors, such as vorinostat, panobinostat, and romidepsin, act as radiosensitizers in brain cancer patients, including those with GBM. These findings suggested that HDAC inhibitors may also act as a chemosensitizer in GBMs. Because vorinostat monotherapy is insufficient to cure GBMs, clinical trials are testing combinations of vorinostat with other drugs. A clinical trial of another HDAC inhibitor, panobinostat, was terminated, whereas romidepsin was the second HDAC inhibitor approved by the U.S. Food and Drug Administration (FDA) for the treatment of patients with refractory cutaneous T-cell lymphoma (CTCL) and peripheral T-cell lymphoma (PTCL). Moreover, romidepsin was found to induce apoptosis in GBM cells[6),7)].

Melatonin is an antioxidant produced in various organs, including the pineal gland, peripheral reproductive tissues, placenta, and ovaries. Melatonin was found to have synergistic apoptotic effects, suggesting that it may be a potential adjuvant in chemotherapy due to its synergistic apoptotic effects[8-18)]. Moreover, melatonin was

observed to synergize with chemotherapeutic drugs in human Ewing sarcoma cells and with HDAC inhibition to induce apoptotic cell death. These findings strongly suggested that melatonin and a HDAC inhibitor might have synergistic therapeutic effects in GBMs and GSCs[16),19)].

GBM cells have been reported to be resistant to apoptosis during chemotherapy of GBM patients. Efforts to identify tumor resistance-related genes in GBM have suggested the involvement of transcription factor EB (TFEB), a master regulator of autophagy that contains helix-loop-helix (HLH) and leucine zipper (LZ) domains. Structural analysis has shown that TFEB undergoes oligomerization, forming tetramers in the presence of DNA and dimers in its absence[20)]. Although misfolded proteins have normal catalytic domains, their activity may be lost. TFEB affects the degradation of misfolded proteins for proteostasis via trafficking[21)] and, following translocation to the nucleus, transcriptionally regulates most lysosomal genes. TFEB overexpression also induces lysosomal biogenesis and degradation via autophagy. For example, TFEB overexpression induces the degradation of glycosaminoglycans and pathogenic proteins that cause neurodegenerative diseases[22)]. Moreover, transcriptome analysis showed an association between TFEB and drug resistance of ovarian cancers[23),24)]. TFEB has been reported to be activated in renal cell carcinoma and non-small cell lung cancer (NSCLC), and to cause renal cell carcinoma via single point mutations. Moreover, increased expression of TFEB was associated with poor prognosis in patients with NSCLC. These findings suggested that TFEB may also be overexpressed and oligomerized in GBMs[25-27)].

As with most cancers, the prevention of recurrence is important in the treatment of GBMs. GSCs, which possess some of the properties of tumor cells, were recently shown to be important for GBM recurrence. Using current therapies, it is very difficult to eliminate GSC subpopulations, including in GBMs[28-31)]. Vorinostat and melatonin may inhibit the proliferation of GSCs by inhibiting the expression and oligomerization of TFEB. Recently, melatonin was reported to reduce the tumorigenicity of GSCs by blocking the AKT-EZH2-STAT3 signaling axis. In addition, melatonin-induced ABCG2/BCRP promoter methylation reduced multidrug

resistance in brain tumor stem cells, and melatonin overcame clofarabine resistance in leukemic cell lines[32-35].

This study found that TFEB is overexpressed and oligomerized in GBMs and GSCs, enhancing their tumorigenicity and proliferation. TFEB oligomerization reduced apoptotic cell death induced by cancer therapeutic agents. Co-treatment with vorinostat and melatonin inhibited the expression and oligomerization of TFEB. Therefore, the goals of this study were to investigate the effects of co-treatment with vorinostat and melatonin on cell apoptosis, and to describe a mechanism that regulates TFEB in heterogeneous and malignant GBMs and GSCs.

Material and Method

1. Gene cloning and mapping

The original TFEB clone (hMU004799) was provided from Korea Human Gene Bank, Medical Genomics Research center, KRIBB, Korea. Constructs HA tagged TFEB, mapping constructs were subcloned into the eukaryotic expression vector, pSG5, by using EcoRI(R0101S, NEB) and BamHI(R0136S, NEB). Amino acid substitutions in TFEB were made using the Takara LA taq (RR002A) via PCR. Their sequences were 5'-CGCGAATTCATGGCGTCACGCATAGGG-3'(Full Forward), 5'-CGCGGATCCTCACAGCACATCGCCCTC-3'(Full Reverse), 5'-CAACAGTGCTC CCAATGCCCCCATGGCCATGCTG-3'(Serine 142 point mutation to Alanine), 5'-TGTCATGCATTACATGCTCGGAGGGCCGCCCA-3'(Poly Q deletion), 5'-CGCGAATTCACCCCGGCCATCAATACC-3'(50~476 Amino Acids Forward), 5'-CGCGAATTCGTCACAGCCTCCCTGGT-3'(200~476 Amino Acids Forward), 5'-CGCGAATTCAGCTCCTGCCCTGCGG-3'(210~476 Amino Acids Forward), 5'-CGCGAATTCCGAGAGCTCACAGATGCTG-3'(220~476 Amino Acids Forward), 5'-CGCGAATTCCTGGCCAAGGAGCGGC-3'(230~476 Amino Acids Forward), 5'-CGCGAATTCCACAACTTAATTGAAAGGAGAC-3'(240~476 Amino Acids Forward), 5'-CGCGAATTCAACATCAATGACCGCATCAAG-3'(250~476 Amino Acids Forward), 5'-CGCGAATTCATGCTGATCCCCAAGGCC-3'(260~476 Amino Acids Forward), 5'-CGCGAATTCGTGCGCTGGAACAAGGG-3'(270~476 Amino Acids Forward), 5'-CGCGAATTCGCCTCTGTGGATTACATCC-3'(280~476 Amino Acids Forward), 5'-CGCGAATTCAAGGACCTGCAAAAGTCCAG-3'(290~476 Amino Acids Forward), 5'-CGCGAATTCAACCACTCTCGCCGCCT-3'(300~476 Amino Acids Forward).

2. Cells and reagents

Human 293T, A172, and U87MG cells were maintained in Dulbecco's modified Eagle's medium (DMEM, Hyclone), supplemented with 10% fetal bovine serum (FBS, Hyclone) and 1% antibiotics (Hyclone) at 37^0C under 5% CO_2. These cells were seeded in 60 mm dishes at 60−70% confluence, with fresh medium added 2 h before transfection with 3 ug DNA, according to the manufacturer's protocol for TransIT-2020 Transfection (Mirus Bio LLC). After incubation for 36 h, the cells were harvested. MES 267 and GSC23 cell lines, provided by The University of Texas M. D. Anderson Cancer Center, were cultured in GSC complete medium, consisting of DMEM/F12/Glutamax (Invitrogen) containing B27 supplements (Gibco), heparin (2.5 mg/ml), 20 ng/ml basic fibroblast growth factor (bFGF; Prospec), and 20 ng/ml epidermal growth factor (EGF; Procpec). Growth factors (bFGF and EGF) were added twice a week. After incubation for 72 h, the cells were harvested. Vorinostat, temozolomide, and everolimus were purchased from Selleckchem, and melatonin was purchased from Sigma Aldrich.

3. Nuclear extract and Oligomerization

Cells were washed twice with PBS, trypsinized, and centrifuged at 3000 rpm for 3 min at 4^0C. After decanting the supernatant, the cells were resuspended in 1 ml Sol A buffer [10 mM Tris (pH 7.4), 10 mM KCl, 3 mM $MgCl_2$, 0.5% NP-40, containing protease inhibitor cocktail], incubated for 20 min on ice, and centrifuged at 4000 rpm for 5 min at 4^0C. The supernatant was transferred into another tube (cytosol proteins), and the pellet was resuspended in 200 μl Sol B buffer [20 mM Tris (pH 7.9), 0.42 M NaCl, 0.2 mM EDTA, 10% glycerol, 2 mM DTT, containing protease inhibitor cocktail] using five strokes of a syringe. The suspension was incubated for 20 min on ice and centrifuged at 13,000 rpm for 20 min, and the supernatant (nuclear extract protein) was transferred to another tube. For oligomerization, 50 μg proteins were prepared in RIPA buffer. Aggregation of the molecules was induced by the addition of 0.004% glutaraldehyde (Sigma Aldrich), with gentle stirring at 4 °C for 2 h. Dye was added, and the proteins were separated

by SDS-PAGE.

4. Immunoprecipitation and western blot analysis

Cell extracts were prepared using lysis buffer and incubated with 1 μg HA (MBL) or Flag (Sigma Aldrich) tagged antibody and 20 μL Protein A/G agarose beads (Santa Cruz) overnight at 4°C. Immunoprecipitated proteins were separated on 8% SDS-PAGE gels and transferred to nitrocellulose membranes. The membranes were blocked by incubation for 2 h in 5% (w/v) non-fat Difco™ skim milk (BD) in blocking buffer (1X PBST), washed in 1X PBST, and incubated overnight at 4° C with primary antibody against HA (MBL), Flag (Sigma Aldrich), actin (Sigma Aldrich), tubulin (Calbiochem), TFEB (Bethyl), LC3B (Cell Signaling), or PARP (Cell Signaling). After washing with 1X PBST, the membranes were incubated for 2 h with secondary HRP-conjugated antibody (Thermo Scientific; Marietta, OH, USA).

5. Oncomine™ platform analysis

The expression of TFEB gene in glioblastoma was analyzed and visualized using the Oncomine™ Platform (Thermo Fisher, Ann Arbor, MI; http://www.oncomine.org). TFEB mRNA from clinical specimens of cancer patients was matched with normal patient datasets, consisting of more than 557 samples. Genes with a threshold p value < 0.0001, a 2-fold change, and ranking in the top 10% were selected because these values are analytical and statistically significant. Parameters evaluated included p-values, fold changes, and cancer subtypes.

6. Histone deacetylase (HDAC) activity

HDAC activity was measured using a commercially available kit (Biovision) according to the manufacturer's instructions. Briefly, whole cell lysates were diluted to the same concentration in assay buffer before the addition of a fluorogenic substrate. The reaction mixtures were incubated for 30 min at 37°C. The reaction was halted by adding lysine developer and incubated for 30 min at 37°C. Fluorescence, as a measure of HDAC activity, was determined using a Tristar^2

Multimode Reader (Berthold) with an excitation wavelength of 360 nm and an emission wavelength of 460 nm. In each experiment, triplicate samples of all conditions and treatments were analyzed.

7. Confocal microscopy

Cells grown on confocal dishes (SPL) were fixed in 4% paraformaldehyde for 10 min, permeabilized with 0.3% Triton X-100 for 5 min, and blocked with 10% goat serum albumin for 1 h at room temperature. The cells were incubated overnight at 4°C with anti-TFEB antibody (Bethyl), washed three times with PBS, and incubated for 45 min at room temperature with FITC-labeled goat anti-rabbit IgG (Santa Cruz) secondary antibody. Nuclei were labeled with DAPI (Sigma Aldrich), and the samples were examined by fluorescence microscopy (LSM710, Zeiss).

8. Proliferation assay

Cell proliferation was determined using the CyQuant Direct Cell Proliferation Assay Kit, following the manufacturer's protocol (Life Technologies). Briefly, CyQUANT direct nucleic acid stain and CyQUANT® direct background suppressor I were mixed together, and the same volume was added to each aliquot of cells. The cells were incubated for 60 min at 37°C, and cell proliferation was determined using the Tristar^2 Multimode Reader with excitation and emission wavelengths of 480 nm and 535 nm, respectively. In each experiment, triplicate samples of all conditions and treatments were analyzed.

9. Immunohistochemistry

TMAs were purchased from US Biomax, and mouse and rabbit specific HRP/DAB IHC detection kits were purchased from Abcam, with assays performed according to the manufacturer's instructions. Briefly, TMAs were deparaffinized and treated with 3% hydrogen peroxide to inactivate endogenous peroxidases. The TMAs were subsequently incubated with a protein block, followed by TFEB (Bethyl) or Ki67 (Abcam), dilution 1:250, for 4 hours at 37°C. After washing, the TMAs were

incubated with biotinylated secondary antibody, washed with buffer, and incubated with streptavidin-peroxidase conjugate. Results were visualized with 3,3'-diaminobenzidine tetrahydrochloride (DAB), and images were analyzed using NIH ImageJ 1.45q software (National Institutes of Health) and a compatible specialized plug-in, IHC profiler. IHC profiler is a software module designed for the quantitative evaluation and automated scoring of digital immunohistochemistry images in imageJ.

10. Cell viability assay

Cell viability was determined by the MTT (3-(4,5-dimethylthiazol-2-yl)-2,5-diphenyltertrazolium bromide) (Sigma Aldrich) assay. Briefly cells were seeded in 96-well plates at a density of 3 x 10^4 cells/well. Melatonin (Sigma Aldrich) Temozolomide (Selleckchem), SAHA (Selleckchem), or Everolimus (Selleckchem) was added, and the cells were incubated at 37 ° C for 24 h in a CO_2 incubator. To each well was added a 20 μL aliquot of MTT reagent (Biovision), followed by incubation for 90 min at 37 ° C in a CO_2 incubator. The absorption of each well was measured at 490 nm with a microplate reader (Berthold). All MTT assay results were presented as the mean (±SD) of three independent experiments.

11. Detection of apoptosis

The extent of apoptosis was assessed using FITC Annexin V Apoptosis Detection Kits (Becton Dickinson), according to the manufacturer's protocol. Briefly, cells were detached with trypsin (Hyclone), followed by FITC annexin V staining and analyzed using a FACScanto II cell cytometer (Becton Dickinson).

12. Animal studies

To examine the therapeutic efficacy, we used 6-8 weeks old female nude mice. The MES 267 cells were injected at a concentration of 1 X 10^5cells in 10 ul PBS into the right hemisphere. Melatonin (15 mg/kg/day), Vorinostat (25 mg/kg/day) and vehicle were injected intraperitoneally at 6 pm daily. All treatments continued for

100days. All procedures were performed in accordance with IACUC-approved animal protocol at the University of Ulsan College of Medicine (2017-13-029).

13. Statistical analysis

Statistical analyses were performed using Excel. Cell proliferation, MTT assay results, HDAC activity, quantification of FACS, and quantification of TFEBs in TMA were analyzed by unpaired Student's t-tests, as appropriate. The p value <0.05 was considered statistically significant.

Result

1. TFEB expression is increased in glioblastoma patients.

Firstly, we analyzed TFEB gene expression in human GBMs using the Oncomine database[36](available at http://www.oncomine.org). TFEB gene expression was higher in GBM samples than in normal brain tissue samples (Fig. 1A and 1B), suggesting that TFEB enhances GBM tumor growth. Additionally, TFEB gene expression was validated using the GEPIA database (available at http://gepia.cancer-pku.cn/), and was observed to present a higher expression in 163 GBM tissues than in 207 normal tissues (Fig. 1C).

Figure 1

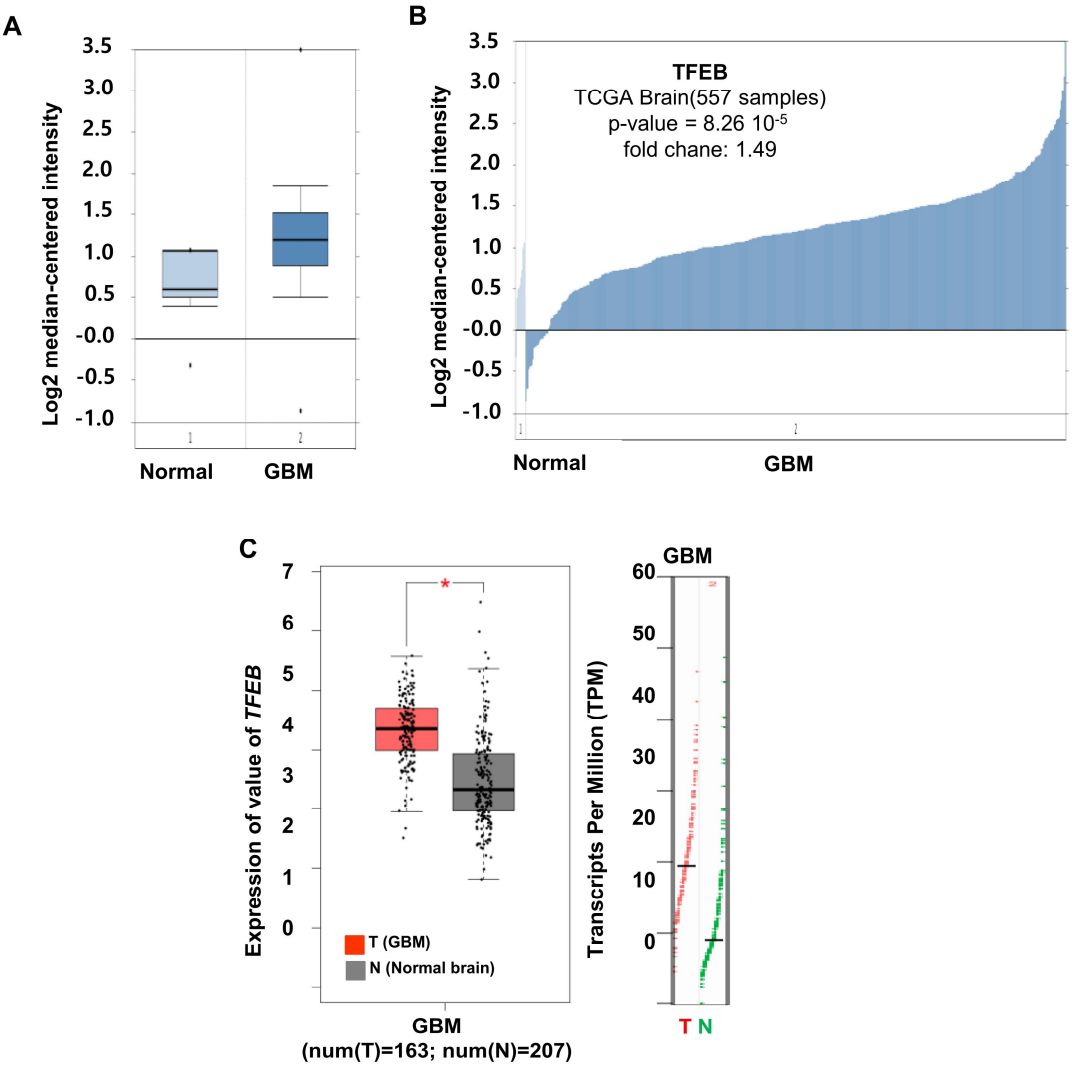
A
Log2 median-centered intensity
3.5
3.0
2.5
2.0
1.5
1.0
0.5
-0.0
-0.5
-1.0
Normal
GBM
B
Log2 median-centered intensity
TFEB
TCGA Brain(557 samples)
p-value = 8.26 10-5
fold chane: 1.49
Normal
GBM
C
Expression of value of TFEB
7
6
5
4
3
2
1
0
T (GBM)
N (Normal brain)
GBM
(num(T)=163; num(N)=207)
GBM
Transcripts Per Million (TPM)
60
50
40
30
20
10
0
T N

Figure 1. TFEB is expressed in aggressive glioblastoma patients.

(A) Box plots derived from gene expression data in Oncomine comparing expression of a specific TFEB gene in normal brain tissue (left plot) and glioblastoma (right plot). (B) TFEB gene expression levels in normal (left plot) and glioblastoma (right plot) evaluated with the Oncomine database. (C) Expression of TFEB gene was detected in 163 GBM tissues (T) and 207 normal tissues (N) from GEPIA. TFEB was overexpressed in GBM tissues than in normal tissues. Axis units are Log2 (TPM+1).

2. Differences in expression levels of TFEB protein in cancer cells and normal cells via IHC.

IHC staining analysis of TFEB proteins in tissue microarrays (TMA) of human GBM and normal brain tissues showed that the level of TFEB protein expression was significantly higher in TMAs of patients with stages III and IV GBM than in TMAs of normal brain tissue, but did not differ significantly in TMAs of patients with early stage GBM and TMAs of normal brain tissues. The tumor proliferation marker Ki67 showed similar patterns (Fig. 2A and 2B).

Figure 2

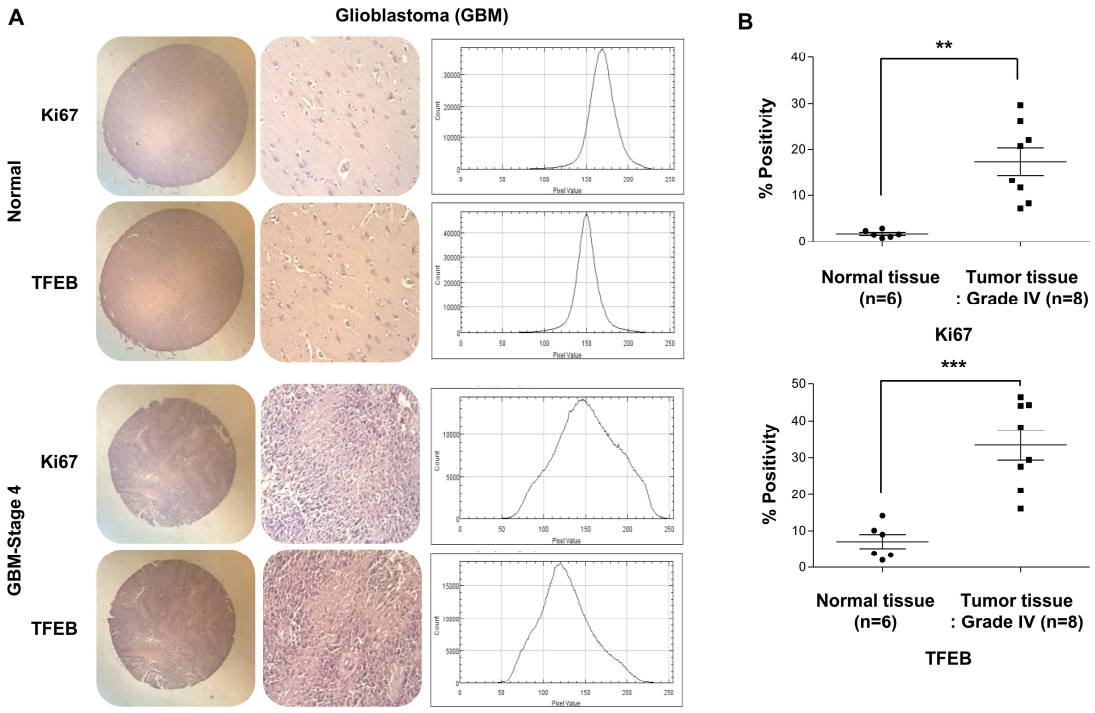
A
Glioblastoma (GBM)
Normal
Ki67
TFEB
GBM-Stage 4
Ki67
TFEB
B
**
% Positivity
Normal tissue (n=6)
Tumor tissue : Grade IV (n=8)
Ki67
***
% Positivity
Normal tissue (n=6)
Tumor tissue : Grade IV (n=8)
TFEB

Figure 2. Differences in expression levels of TFEB protein in cancer cells and normal cells via IHC.

(A, B) Immunohistochemical (IHC) analysis of tissue microarrays (TMAs) for human normal brain and glioblastoma tissue samples using anti-TFEB and Ki67 antibodies. Data were analyzed using an IHC profiler. Each group consisted of 6 samples and statistical processing was performed through excel. $*P < 0.005$.

3. Expression of TFEB protein in glioblastoma cell lines.

Immunoblotting assay with anti-TFEB antibody showed that TFEB was expressed and formed homo-oligomers in the human GBM cell lines, including A172, LN18, LN229, T98G, U87MG, U118, U343 and U373 cells, with the highest levels of expression observed in A172 and U87MG cells (Fig. 3). Moreover, the higher molecular weight bands observed in A172 and U87MG cells likely represent TFEB oligomers. These findings suggested that TFEB is highly expressed in aggressive GBMs.

Figure 3

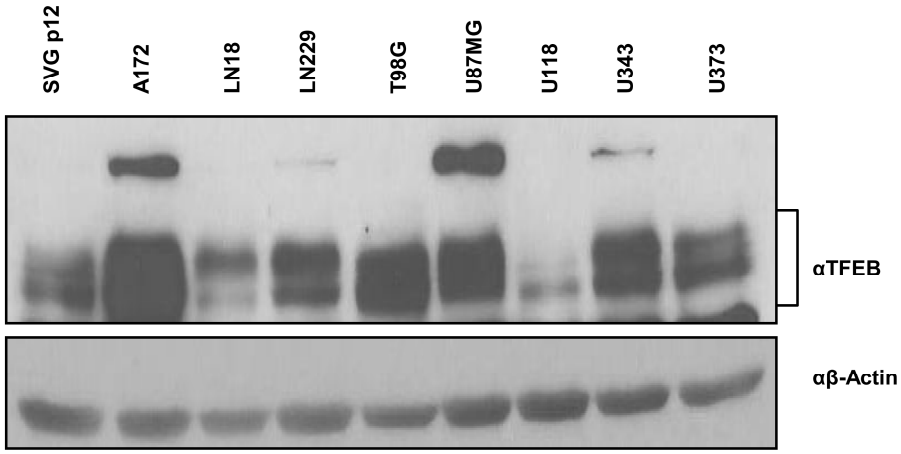
SVG p12
A172
LN18
LN229
T98G
U87MG
U118
U343
U373
αTFEB
αβ-Actin

Figure 3. Expression of TFEB protein in glioblastoma cell lines.

Levels of TFEB protein expression in lysates of human glioblastoma cells. Whole cell lysates were immunoblotted by anti-Actin and anti-TFEB antibodies.

4. Vorinostat induces apoptosis of human GBM cells which had resistant about anti-cancer drug.

Next, we tested the effects of the chemotherapy reagents, temozolomide (TMZ) and everolimus (EVM), on the viability of GBM cells expressing various levels of TFEB. We found that the treatment of these cells with 100 μM TMZ or 4 μM EVM for 24 h had little effect on cell viability (Fig. 4A and 4B), indicating that GBM cells are resistant to apoptosis-inducing agents. This lack of effect may be due to the overexpression of O-6-methylguanine methyltransferase (MGMT) or the loss of a DNA repair system in GBM cells.

Epigenetic regulation in human cancers, including GBM, may be a treatment target. HDAC inhibitors may be effective in treating aggressive cancers, including GBM. Phase II clinical trials are currently testing combinations of the HDAC inhibitor vorinostat (SAHA) with targeted agents, TMZ and radiotherapy, in various types of cancer, including GBM. To assess the effects of HDAC inhibitors on the proliferation of GBM cells, cells were treated with a HDAC inhibitor (vorinostat, panobinostat and mocetinostat), TMZ or EVM. We found that the HDAC inhibitors vorinostat and mocetinostat effectively reduced the cell survival of U89MG and A172 cells, whereas another HDAC inhibitor, panobinostat, did not (Fig. 4C and 4D).

Figure 4

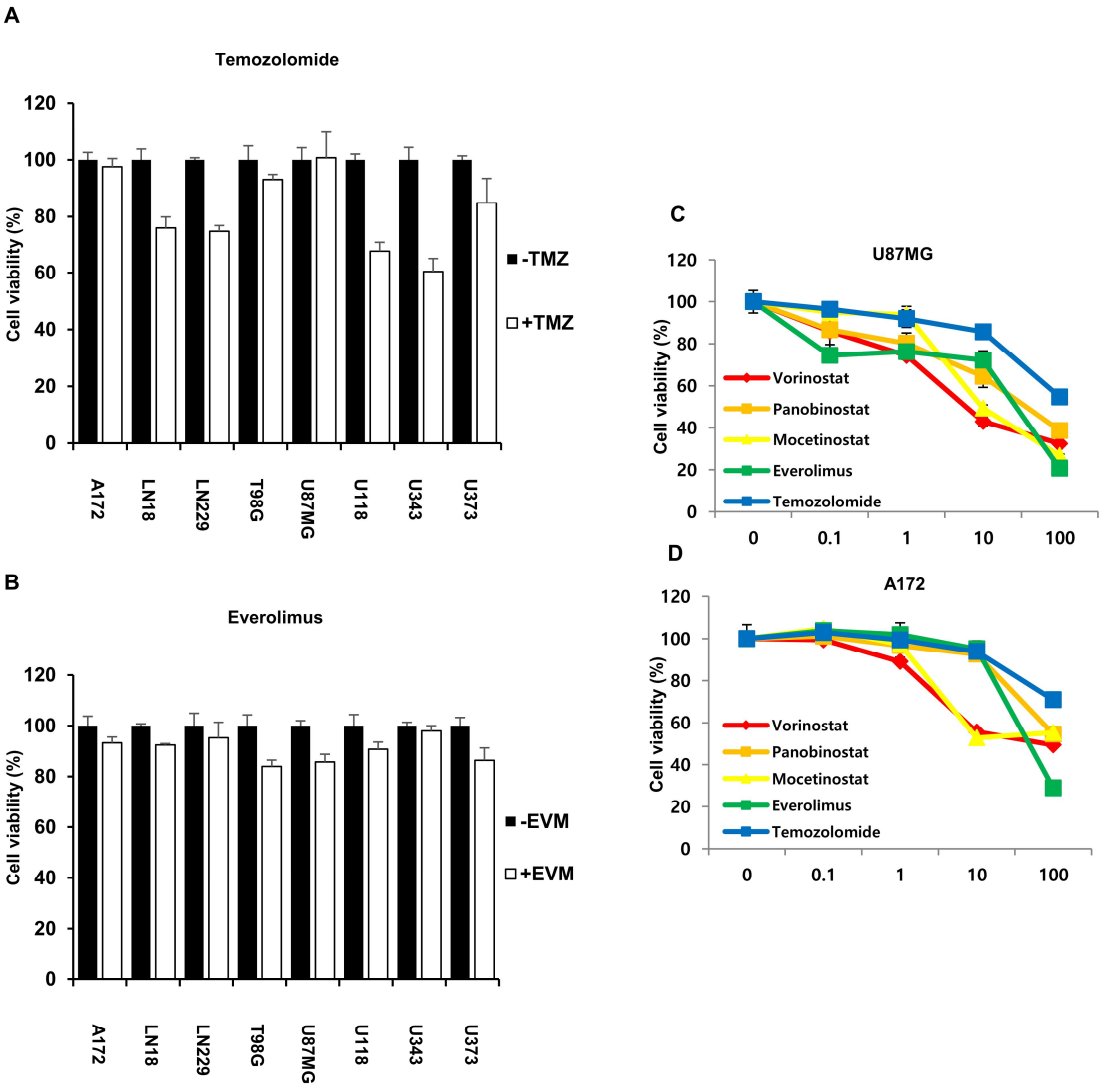
A
Temozolomide
Cell viability (%)
120
100
80
60
40
20
0
A172
LN18
LN229
T98G
U87MG
U118
U343
U373
-TMZ
+TMZ
B
Everolimus
Cell viability (%)
-EVM
+EVM
C
U87MG
Cell viability (%)
Vorinostat
Panobinostat
Mocetinostat
Everolimus
Temozolomide
0
0.1
1
10
100
D
A172
Cell viability (%)
Vorinostat
Panobinostat
Mocetinostat
Everolimus
Temozolomide

Figure 4. Vorinostat induces apoptosis of human GBM cells which had resistant about anti-cancer drug.

(A) and (B) Human glioblastoma cells were treated with (A) 100 μM temozolomide or (B) 4 μM everolimus for 24 hr. Each column was normalized relative to vehicle. Cell viability was determined by MTT assays. Each experiment was repeated at least three times, and the data were expressed as mean±SE of the mean. (C) U87MG and (D) A172 cells were treated with various drugs as indicated (concentration of TMZ is X10, as indicated), and cell viability was determined by MTT assays. Each experiment was repeated at least three times, and the data were expressed as mean±SE of the mean.

5. Vorinostat decreases the TFEB expression and TFEB oligomerization.

Treatment with vorinostat resulted in the cleavage of PARP and reduced TFEB proteins in both U87MG and A172 cells (Fig. 5A). HDAC activity also measured that vorinostat significantly reduced HDAC activity in U87MG cells by using HDAC assay kits (Biovision) (Fig. 5B), suggesting that vorinostat may have therapeutic activity in GBM cells.

To demonstrate the biological functions that TFEB undergoes oligomerization, forming tetramers for the role of transcription factor[20], we firstly assessed the oligomerization of TFEB in U87MG cells and inhibition by vorinostat (Fig. 5C). Glutaraldehyde is a well-known reagent in the study of structural and chemical-related functions of proteins and cross-linking reagents.

Figure 5

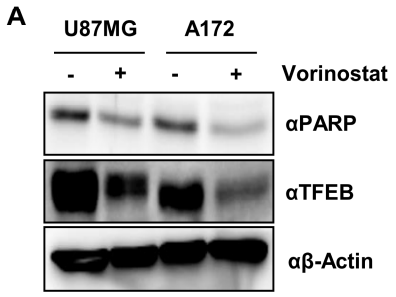
A
U87MG
A172
- + - +
Vorinostat
αPARP
αTFEB
αβ-Actin

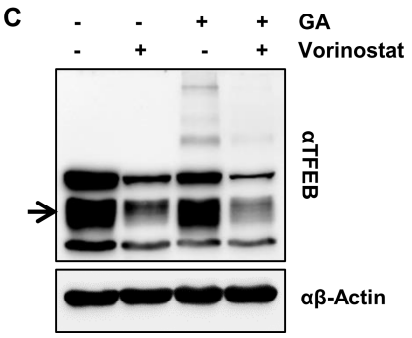
C
- - + + GA
- + - + Vorinostat
αTFEB
αβ-Actin

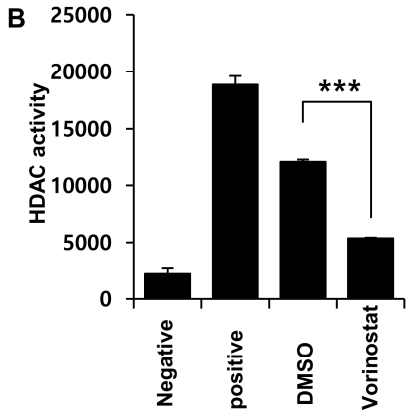
B
25000
20000
15000
10000
5000
0
HDAC activity
***
Negative
positive
DMSO
Vorinostat

Figure 5. Vorinostat decreases the TFEB expression and TFEB oligomerization.

(A) U87MG and A172 cells were treated with 8 μM vorinostat or vehicle for 24 hr, and the levels of TFEB, PARP, and β-actin proteins were assayed by western blotting. (B) U87MG cells were treated with 8 μM vorinostat or vehicle for 24 hr, and HDAC activity was measured using a fluorometric assay kit. $*P < 0.005$. (C) U87MG cells were treated with 8 μM vorinostat or vehicle for 24 hr. Whole cell lysates were incubated in the presence or absence of glutaraldehyde, and the levels of TFEB and β-actin proteins were assayed by western blotting.

6. TFEB depletion promotes vorinostat mediated apoptosis and TFEB oligomerization.

Also, to determine whether inhibition of TFEB oligomerization increased vorinostat sensitivity and induced apoptosis in GBM cells, we generated TFEB-depleted U87MG cells using lentiviral TFEB shRNA (Fig. 6A). Thus, we also found that TFEB-depletion inhibited TFEB oligomerization in U87MG cells (Fig. 6B), and vorinostat induced PARP cleavage in these TFEB-depleted U87MG cells. In addition, vorinostat enhanced the phosphorylation of H2AX, an indicator of DNA double-strand breaks and subsequent apoptosis (Fig. 6C). Vorinostat suppressed TFEB oligomerization in parent U89MG cells, with no evidence of oligomerization in TFEB-depleted U89MG cells (Fig. 6D). These results suggest that the oligomerization of TFEB leads to increased GBM cell proliferation and tumorigenicity, ultimately overcoming the inhibition of apoptosis by vorinostat.

Figure 6

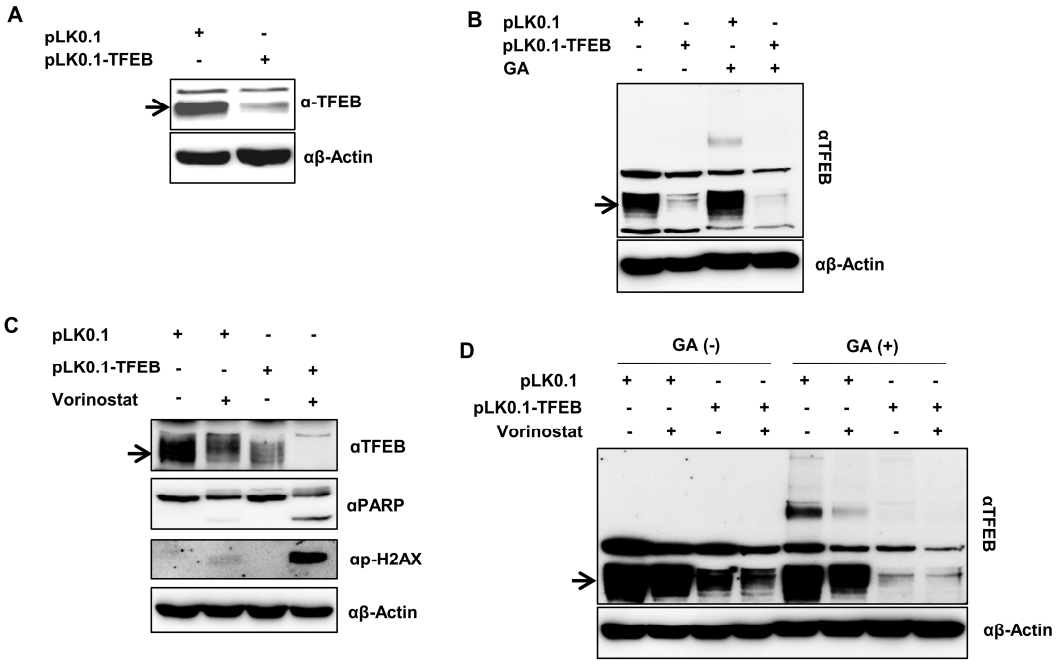
A
pLK0.1 + -
pLK0.1-TFEB - +
α-TFEB
αβ-Actin
B
pLK0.1 + - + -
pLK0.1-TFEB - + - +
GA - - + +
αTFEB
αβ-Actin
C
pLK0.1 + + - -
pLK0.1-TFEB - - + +
Vorinostat - + - +
αTFEB
αPARP
αp-H2AX
αβ-Actin
D
GA (-)
GA (+)
pLK0.1 + + - - + + - -
pLK0.1-TFEB - - + + - - + +
Vorinostat - + - + - + - +
αTFEB
αβ-Actin

Figure 6. TFEB depletion promotes vorinostat mediated apoptosis and TFEB oligomerization.

(A) U87MG cells infected with pLK0.1 or pLK0.1-TFEB. Whole cell lysates were used for immunoblotted by anti-TFEB and anti-Actin antibodies. (B) Whole cell lysates of U87MG cells infected with pLK0.1 or pLK0.1-TFEB were incubated in the presence or absence of glutaraldehyde, and the levels of TFEB and β-actin proteins were assayed by western blotting. (C) U87MG cells infected with pLK0.1 and pLK0.1-TFEB were treated with 8 μM vorinostat or vehicle for 24 hr, and the levels of TFEB, PARP, p-H2AX, and β-actin were determined by western blotting. (D) Whole cell lysates of U87MG cells infected with pLK0.1 and pLK0.1-TFEB treated with 8 μM vorinostat or vehicle for 24 hr were incubated with glutaraldehyde, and the levels of TFEB and β-actin were determined by western blotting.

7. Overexpression of TFEB inhibits vorinostat-induced apoptosis.

To better understand the physiological role of TFEB expression in GBM cells, we examined vorinostat control of apoptosis in TFEB overexpressing U87MG and A172 cells. Vorinostat treatment of TFEB overexpressing U87MG cells showed a lack of PAPR cleavage and an inhibition of caspase-3 activity (Fig. 7A). Vorinostat-treated U87MG cells displayed changes in morphology associated with apoptosis, whereas vorinostat-treated TFEB overexpressing U87MG cells did not (Fig. 7B). In assessing whether vorinostat-induced apoptosis of GBM cells is dependent on TFEB expression, we found that overexpression of TFEB in vorinostat-treated U87MG cells significantly reduced the number of annexin V-positive cells compared with parent U87MG cells (Fig. 7C). Western blot analysis with anti-TFEB and anti-PARP antibodies showed similar results in vorinostat-treated TFEB overexpressing A172 cells (Fig. 7D).

Figure 7

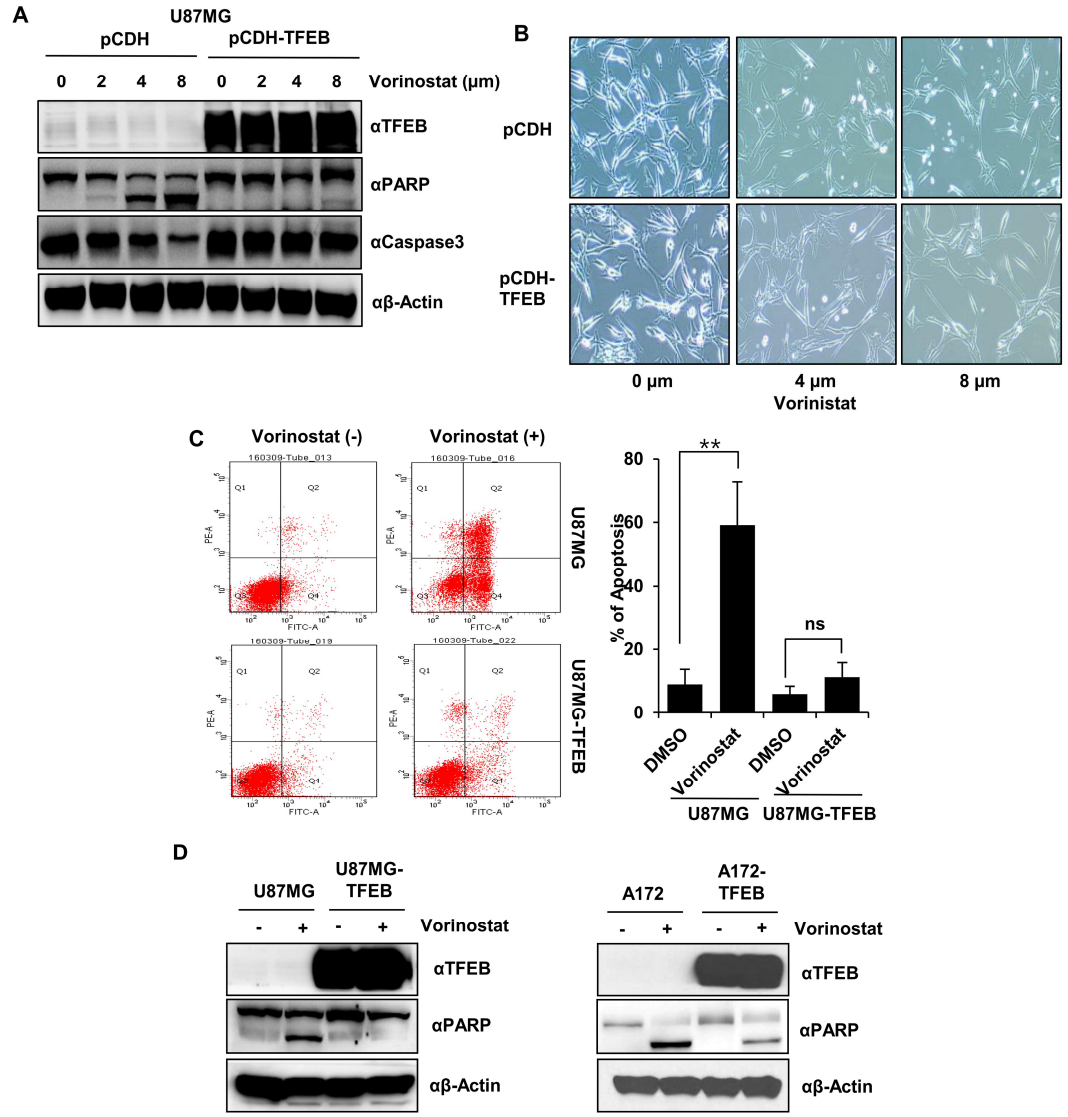
A
U87MG
pCDH
pCDH-TFEB
0 2 4 8 0 2 4 8 Vorinostat (μm)
αTFEB
αPARP
αCaspase3
αβ-Actin
B
pCDH
pCDH-TFEB
0 μm
4 μm
Vorinistat
8 μm
C
Vorinostat (-)
Vorinostat (+)
U87MG
U87MG-TFEB
% of Apoptosis
**
ns
DMSO
Vorinostat
DMSO
Vorinostat
U87MG
U87MG-TFEB
D
U87MG
U87MG-TFEB
A172
A172-TFEB
- + - + Vorinostat
αTFEB
αPARP
αβ-Actin

Figure 7. Overexpression of TFEB inhibits vorinostat-induced apoptosis.

(A) U87MG cells infected with pCDH or pCDH-TFEB were treated with the indicated concentrations of vorinostat for 24 hr. Protein levels of TFEB, PARP, caspase3, and β-actin were determined by western blotting. (B) U87MG cells infected with pCDH or pCDH-TFEB were treated with the indicated concentrations of vorinostat for 24 hr. Cell morphology was determined by phase contrast microscopy. (C) U87MG cells infected with pCDH and pCDH-TFEB were treated with 8 μM vorinostat or vehicle for 24 hr, and apoptosis was assayed by FACS. Each experiment was repeated at least three times, and data were expressed as mean±SE of the mean. *$P < 0.005$. (D) U87MG (upper panel) and A172 (lower panel) cells infected with pCDH and pCDH-TFEB were treated with 8 μM vorinostat or vehicle for 24 hr. Western blotting was performed to determine the protein levels of TFEB, PARP, and β-actin.

8. TFEB mediated transcriptional change of apoptotic genes.

To examine the transcriptional activity of pro-apoptosis target genes, NOXA and PUMA, we performed qPCR analysis in parent U87MG and TFEB overexpressing U87MG cells. The transcriptional activities of NOXA and PUMA were increased by vorinostat-mediated apoptosis in parent, but not in TFEB overexpressing, U87MG cells, suggesting that TFEB overexpression significantly inhibited the transcription of these genes (Fig. 8A). Taken together, these results demonstrate that TFEB overexpression attenuated the effects of vorinostat-induced apoptosis signaling, resulting in the transcriptional repression of pro-apoptotic target genes, including . Concomitantly, we observed that vorinostat altered the nuclear translocation of TFEB, as shown by fractionation analysis of both U87MG and TFEB overexpressing U87MG cells. Vorinostat had little effect on the levels of TFEB in the cytoplasm and nucleus of U87MG cells (Fig. 8B).

Figure 8

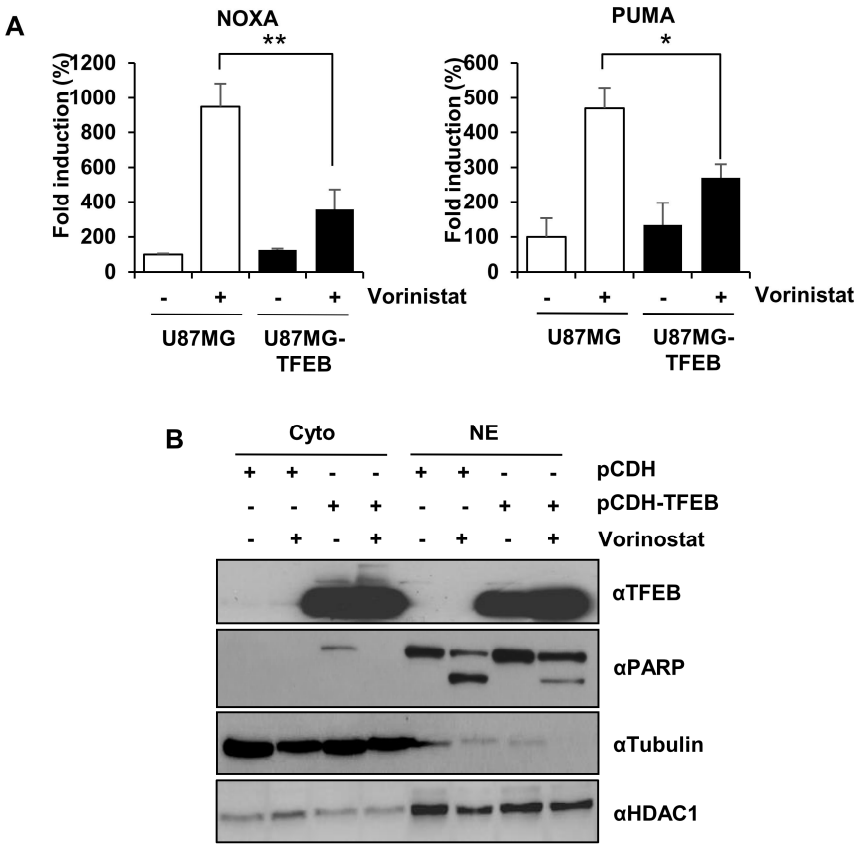
A
NOXA
**
Fold induction (%)
1200
1000
800
600
400
200
0
- + - +
Vorinistat
U87MG
U87MG-TFEB
PUMA
*
Fold induction (%)
600
500
400
300
200
100
0
- + - +
Vorinistat
U87MG
U87MG-TFEB
B
Cyto
NE
+ + - - + + - - pCDH
- - + + - - + + pCDH-TFEB
- + - + - + - + Vorinostat
αTFEB
αPARP
αTubulin
αHDAC1

Figure 8. TFEB mediated transcriptional change of apoptotic genes.

(A) U87MG cells infected with pCDH and pCDH-TFEB were treated with vorinostat or vehicle for 24 hr. Real-time RT-PCR was performed to analyze NOXA and PUMA mRNAs expression. The data were expressed as mean±SE of the mean. Three independent experiments were performed. $*P < 0.005$. (B) U87MG cells infected with pCDH and pCDH-TFEB were treated with vorinostat or vehicle for 24 hr. Their nuclei were extracted and subjected to western blotting to determine the protein levels of TFEB, PARP, tubulin, and HDAC1.

9. Oligomerization and nuclear translocation of TFEB in human glioblastoma cells.

TFEB contains HLH and LZ domains, both of which facilitate protein homo- or hetero-oligomerization with proteins containing these domains. Although TFEB efficiently oligomerizes[37], its oligomerization and translocation into the nucleus of GBM cells are incompletely understood. To investigate the TFEB domains critical for oligomerization, we cloned the TFEBD210, TFEBD240, and TFEBD290 fragments, And we examined whether nuclear translocation of TFEB occurs in U87MG and A172 human GBM cells (Fig. 4A and 4B). As expected, TFEB amino acids 210–476 translocated into the nucleus, whereas amino acids 240–476 did not. To confirm the translocation of TFEB domains in GBM cells, we performed immunofluorescence (IF) assays using confocal microscopy. We found that wild-type TFEB and TFEB amino acids 210–476 were present in the nuclei of U87MG cells (Fig. 4C). To support the function of the oligomerized-TFEB domains by vorinostat, PARP cleavage was measured by immunoblotting assay. The indicated TFEB domains were overexpressed in U87MG cells. As expected, TFEB amino acids 290-476 didn't inhibit the vorinostat-induced apoptosis (Fig. 4D). Taken together, these results confirmed that amino acids 230–239 were required for nuclear translocation of TFEB and that nuclear translocation and oligomerization of TFEB is necessary for its activity as a transcription factor.

Figure 9

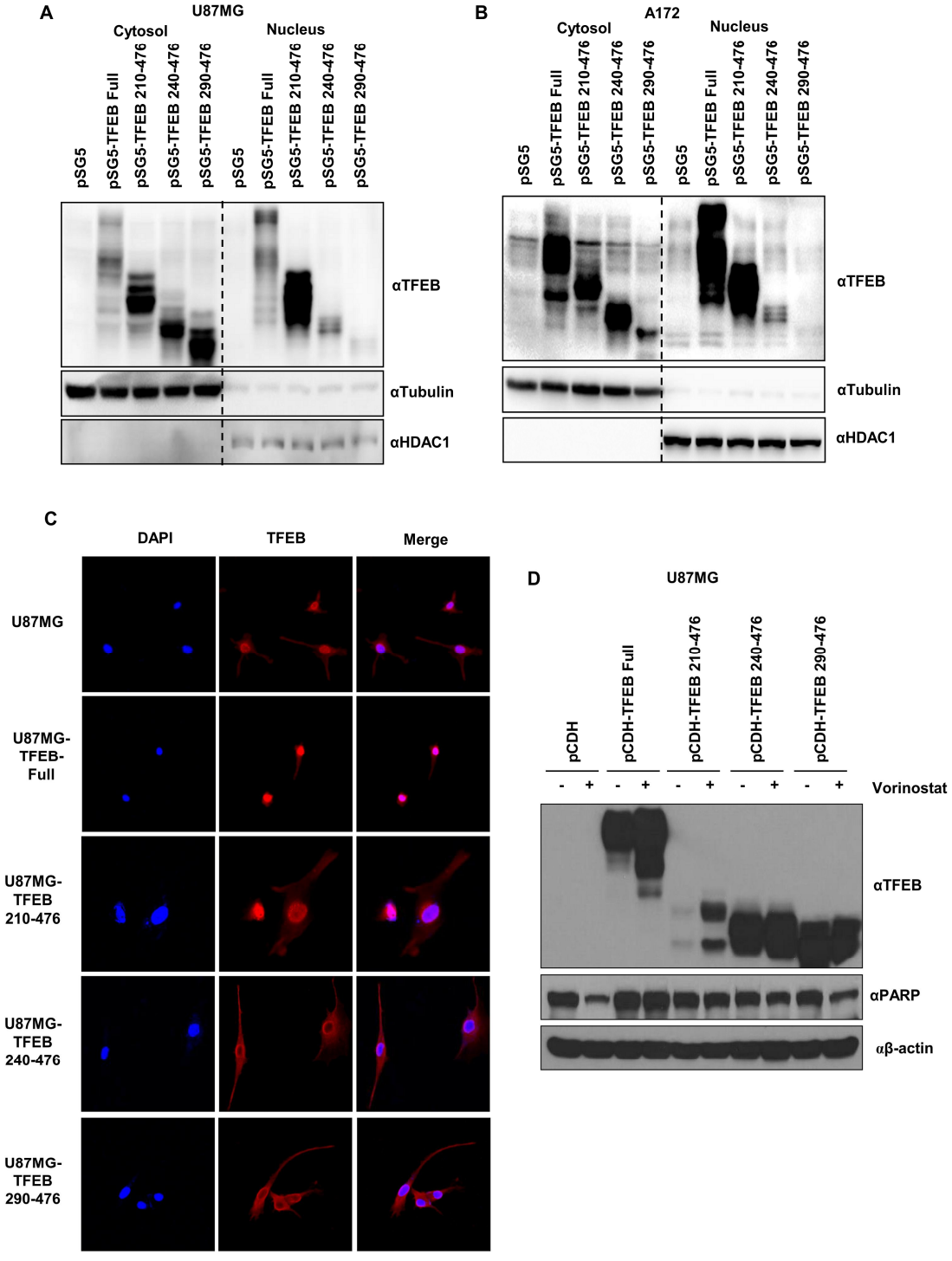
A
U87MG
Cytosol
Nucleus
pSG5
pSG5-TFEB Full
pSG5-TFEB 210-476
pSG5-TFEB 240-476
pSG5-TFEB 290-476
αTFEB
αTubulin
αHDAC1
B
A172
C
DAPI
TFEB
Merge
U87MG
U87MG-TFEB-Full
U87MG-TFEB 210-476
U87MG-TFEB 240-476
U87MG-TFEB 290-476
D
U87MG
pCDH
pCDH-TFEB Full
pCDH-TFEB 210-476
pCDH-TFEB 240-476
pCDH-TFEB 290-476
Vorinostat
αPARP
αβ-actin

Figure 9. Nuclear translocation of oligomerized-TFEB in human glioblastoma cells.

Nuclear extracts were obtained from (A) U87MG and (B) A172 cells transfected with the indicated vectors, and protein levels of TFEB, tubulin, and HDAC1 were determined by western blotting. (C) U87MG cells transfected with the indicated vectors and subjected to immunofluorescence staining for TFEB (red) were visualized by confocal microscopy. Nuclei were stained with DAPI. (D) U87MG cells infected with as indicated were treated with Vorinostat 8um for 24hr, and protein levels of PARP and β-actin were determined by western blotting.

10. Melatonin specifically inhibits proliferation and survival in glioblastoma.

In addition to being a major pineal secretory product, melatonin is produced in extrapineal organs, including the retina, skin, lymphocytes, bone marrow, thymus, and ovary[38-41]. Recently, melatonin has been reported to inhibit tumor proliferation and tumorigenicity[33]. To assess the roles of melatonin in GSC and GBM cells, we analyzed TFEB expression in GBM cells, finding that melatonin dose-dependently reduced TFEB protein levels in U87MG cells, but not in SVGp12 cells, a line of control normal brain-human fetal glial cells (Fig. 10A). Low concentrations (0−0.5 mM) of melatonin, however, had little effect on the expression of TFEB proteins in U87MG cells (Fig. 10B). Melatonin also reduced the proliferation (Fig. 10C) and viability (Fig. 10D) of U87MG, but not of SVGp12, cells. These results suggest that melatonin attenuates GBM cell proliferation and TFEB expression.

Figure 10

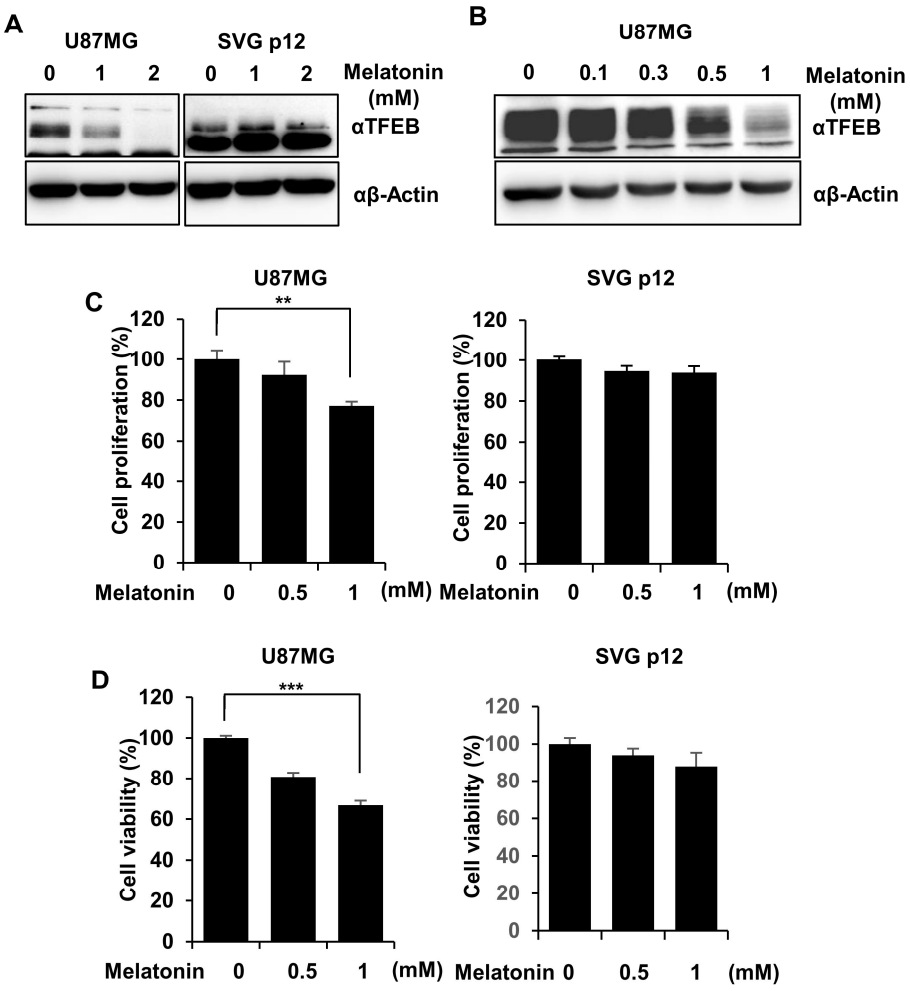
A
U87MG
SVG p12
0 1 2 0 1 2
Melatonin (mM)
αTFEB
αβ-Actin
B
U87MG
0 0.1 0.3 0.5 1
Melatonin (mM)
αTFEB
αβ-Actin
C
U87MG
SVG p12
**
Cell proliferation (%)
120
100
80
60
40
20
0
Melatonin 0 0.5 1 (mM)
D
U87MG
SVG p12
***
Cell viability (%)
120
100
80
60
40
20
0
Melatonin 0 0.5 1 (mM)

Figure 10. Melatonin specifically inhibits proliferation and survival in glioblastoma.

(A) U87MG and SVGp12 cells were treated with the indicated concentrations of melatonin for 48 hr and subjected to western blotting to determine the protein levels of TFEB and β-actin. (B) U87MG cells were treated with the indicated concentrations of melatonin for 48 hr and subjected to western blotting to determine the protein levels of TFEB and β-actin. (C) U87MG and SVG p12 cells were treated with the indicated concentrations of melatonin for 48 hr and subjected to cell proliferation assays. Each condition was repeated at least three times, and the data were expressed as mean±SE of the mean. (D) U87MG cells were treated with the indicated concentrations of melatonin for 48 hr, and cell viability was determined by MTT assays. Each condition was repeated at least three times, and the data were expressed as mean±SE of the mean. $*P < 0.05$

11. Co-treatment of melatonin and vorinostat effectively induced apoptosis of human glioblastoma cells.

We therefore examined whether co-treatment with melatonin and vorinostat could efficiently induce GBM cell apoptosis by reducing TFEB proteins. As expected, treatment with both vorinostat and melatonin reduced TFEB expression, while synergistically increasing cleaved PARP and active (cleaved) caspase-3 and p-γ H2AX (Fig. 11A), reducing GBM cell viability (Fig. 11B). Although treatment with either melatonin or vorinostat alone partially inhibited the oligomerization of TFEB proteins, their combination completely inhibited the oligomerization and expression of TFEB proteins (Fig. 11C). These findings indicate that co-treatment with vorinostat and melatonin efficiently enhanced cell death by inhibiting TFEB expression in GBM cells.

Figure 11

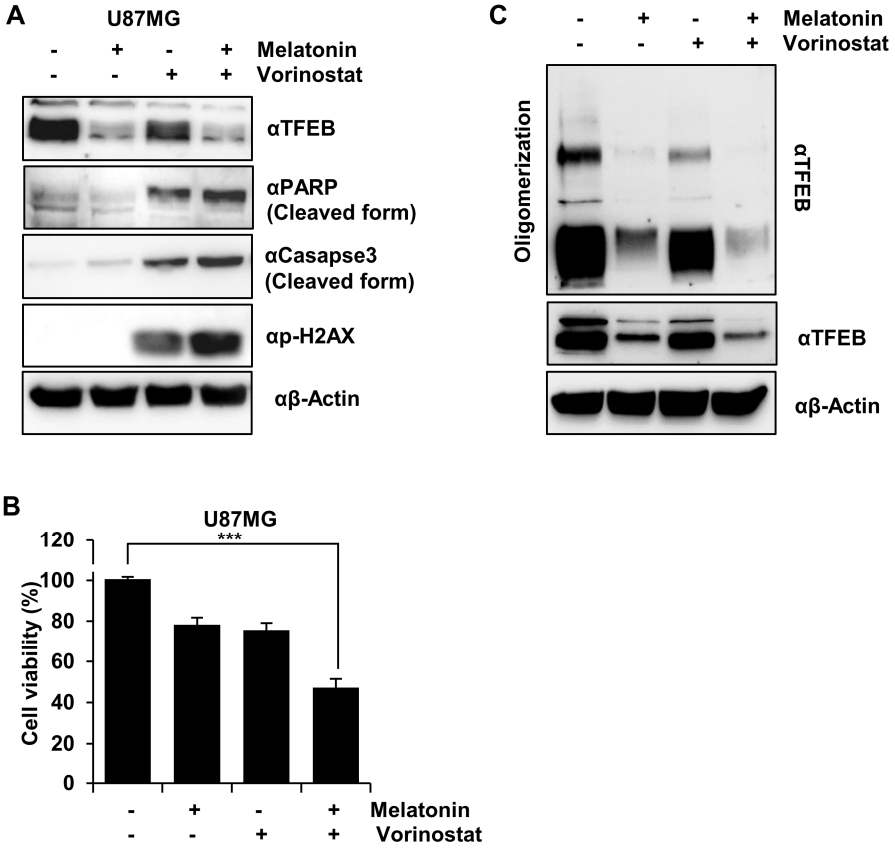
A
U87MG
- + - + Melatonin
- - + + Vorinostat
αTFEB
αPARP
(Cleaved form)
αCasapse3
(Cleaved form)
αp-H2AX
αβ-Actin
C
- + - + Melatonin
- - + + Vorinostat
Oligomerization
αTFEB
αTFEB
αβ-Actin
B
U87MG
***
Cell viability (%)
120
100
80
60
40
20
0
- + - + Melatonin
- - + + Vorinostat

Figure 11. Co-treatment of melatonin and vorinostat effectively induced apoptosis of human glioblastoma cells.

(A) U87MG cells were treated with 1 mM melatonin and 8 μM vorinostat for 48 hr. Western blotting was performed to determine the protein levels of TFEB, PARP, caspase-3, p-H2AX, and β-actin. (B) U87MG cells were treated with 1 mM melatonin and 8 μM vorinostat for 48 hr, and cell viability was determined by MTT assays. Each condition was repeated at least three times, and data were expressed as mean±SE of the mean. *$P < 0.005$ (C) Whole cell lysates of U87MG cells treated with 1 mM melatonin and 8 μM vorinostat for 48 hr were incubated in the presence or absence of glutaraldehyde. Western blotting was performed to determine the protein levels of TFEB and β-actin.

12. Melatonin synergistically enhances vorinostat-mediated apoptosis in human glioma stem cells (GSCs).

Most human GBMs are characterized by heterogeneous tumor cell populations, which include GSCs. GSC heterogeneity has been reported to contribute to treatment resistance[42-44]. The effects of vorinostat and melatonin on the proliferation and apoptosis of GSCs were therefore tested using the primary human GSC cell lines MES 267 and GSC23 (Fig. 12A and Fig. 12E). We found that treatment with vorinostat and melatonin dramatically reduced sphere formation by MES 267 and GSC23 cells compared with untreated control GSCs. Sphere counting and proliferation analysis also showed that treatment with vorinostat and melatonin reduced the number and proliferation of tumor spheres (Fig. 12B and 12C, and Fig. 12F and 2G). Co-treatment of MES 267 cells with vorinostat and melatonin reduced the expression of TFEB, while increasing the expression of cleaved PARP and phosphorylated γH2AX (Fig. 12D and Fig. 12H). These results suggest that melatonin synergizes with vorinostat to enhance apoptosis in GSCs by inhibiting tumor-sphere formation (Fig. 12).

Figure 12

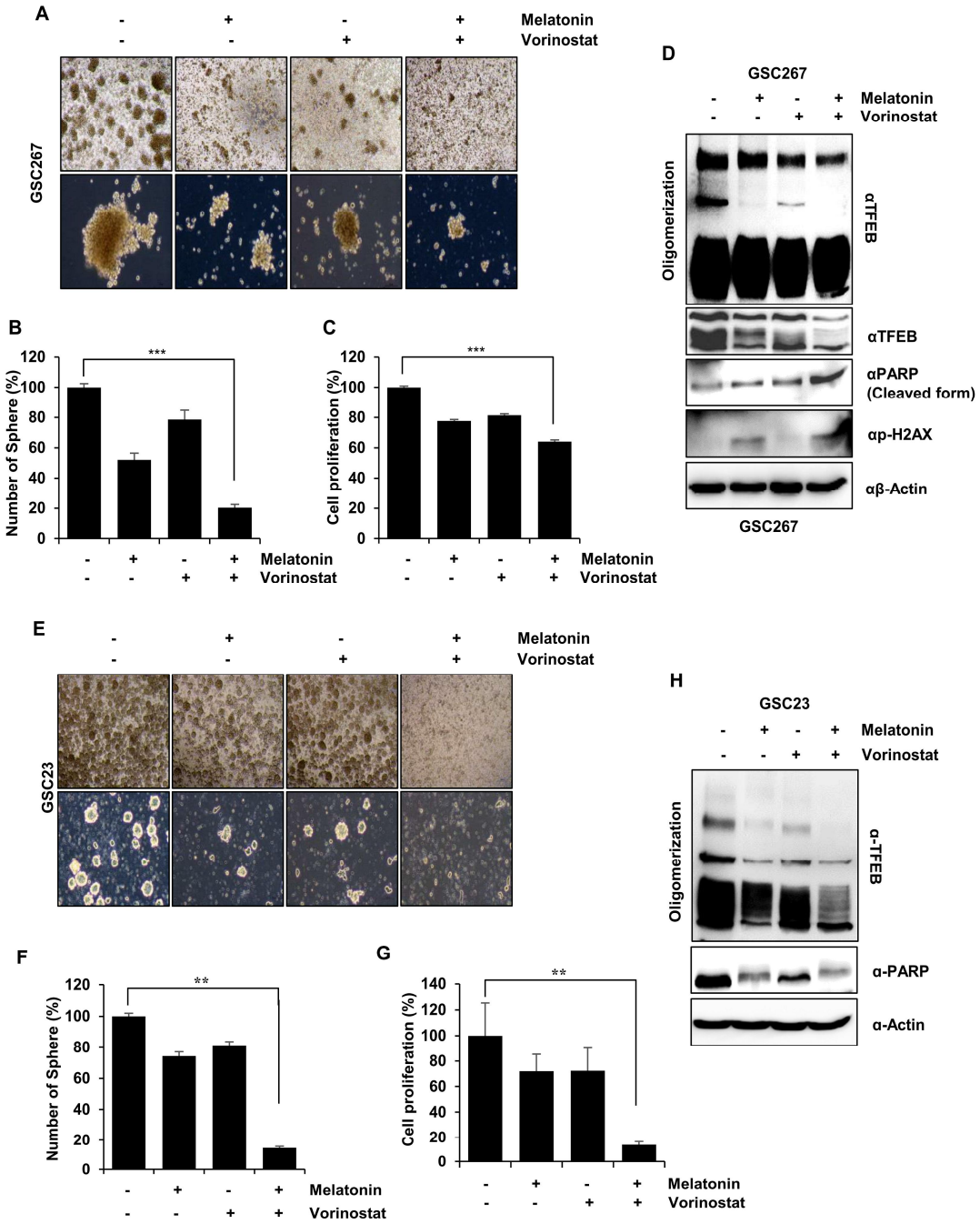
A
Melatonin
Vorinostat
GSC267
B
Number of Sphere (%)
C
Cell proliferation (%)
D
GSC267
Oligomerization
αTFEB
αPARP
(Cleaved form)
αp-H2AX
αβ-Actin
E
GSC23
F
G
H
α-TFEB
α-PARP
α-Actin

Figure 12. Melatonin synergistically enhances vorinostat-mediated apoptosis in human glioma stem cells (GSCs).

(A, E) GSC 267 cells and GSC23 cells were treated with 1 mM melatonin and 4 μM vorinostat for 72 hr, and cell morphology was determined by phase contrast imaging. (B, F) Tumor-sphere-forming ability of GSC 267 cells and GSC23 cells was determined by counting spheres. $*P < 0.005$ (C, G) Proliferation assays were performed to determine cell proliferation. $*P < 0.005$ (K, H) Whole cell lysates of GSC 267 cells and GSC23 cells treated with 1 mM melatonin and 4 μM vorinostat for 72 hr were incubated in the presence or absence of glutaraldehyde. Western blotting was performed to determine the protein levels of TFEB, PARP, p-H2AX, and β-actin.

13. Co-treatment of melatonin and vorinostat effectively overcome drug resistance by TFEB and induces apoptosis.

To determine whether the effect of co-treatment overcome the TFEB mediated drug resistance, we established TFEB overexpressing GSC 267. And we performed the melatonin and vorinostat co-treatment at GSC 267 pCDH or pCDH-TFEB infected. As we expected, co-treatment of melatonin and vorinostat can induce total PARP cleavage at the both groups (Fig. 13).

Figure 13

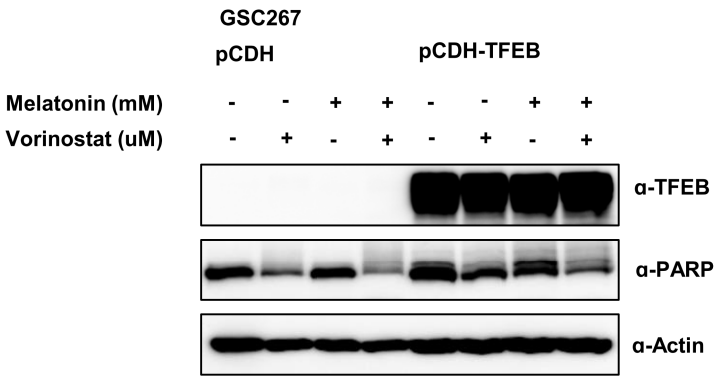
GSC267
pCDH
pCDH-TFEB
Melatonin (mM) - - + + - - + +
Vorinostat (uM) - + - + - + - +
α-TFEB
α-PARP
α-Actin

Figure 13. Co-treatment of melatonin and vorinostat effectively overcome drug resistance by TFEB and induces apoptosis.

GSC 267 cells infect with pCDH or pCDH-TFEB were treated with 1mM melatonin and 4uM vorinostat for 72hr as indicated. Protein levels of TFEB, PARP, β-actin were determined by western blotting.

14. Effect of melatonin and vorinostat treatment on orthotopic xenograft tumor growth and survival.

Next, we investigated whether the co-treatment of melatonin and vorinostat affects in vivo tumorigenic potential using the orthotopic xenograft models. Median survival times of controls and mice treated with melatonin, vorinostat and melatonin+vorinostat (n=6 per each group) were 63, 74, 91 and 106 days (Fig. 13A). After sacrificing mice, mouse brains were sectioned and stained with H&E (Fig. 13B). Combined treatment of melatonin and vorinostat in GSC 267-injected mice brains significantly decreased in vivo tumor growth, thereby prolonging the median survival of the tumor-bearing mice. In contrast, melatonin or vorinostat treatment did not decrease in vivo tumor growth and survival. These results indicate that co-treatment of melatonin and vorinostat significantly sufficient to inhibit tumorigenicity in GSCs.

Figure 14

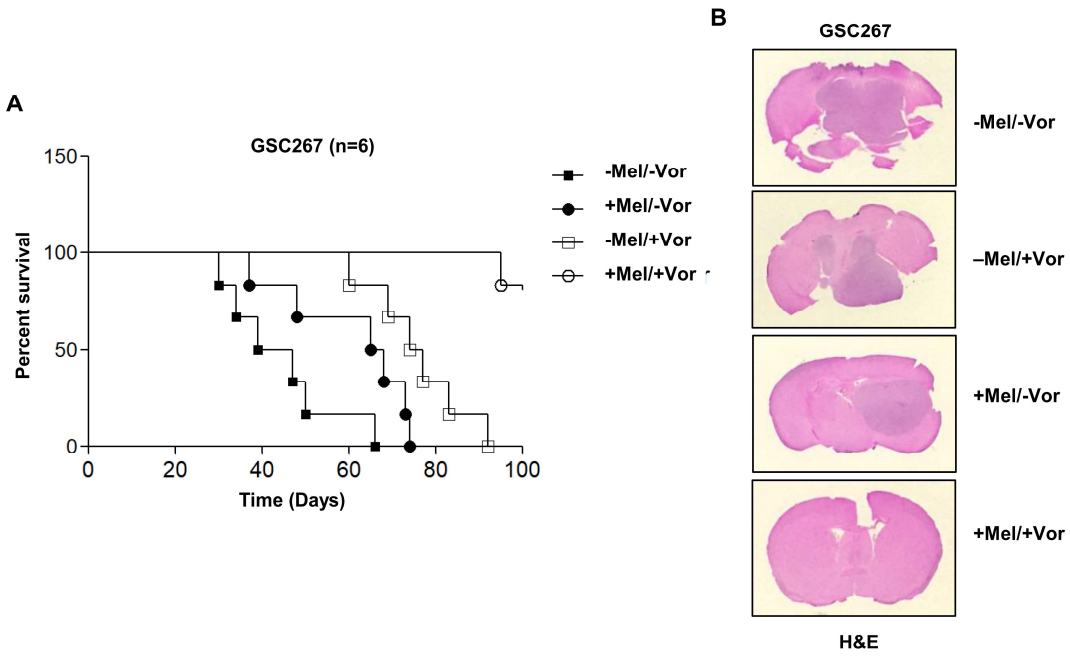
A
GSC267 (n=6)
Percent survival
150
100
50
0
0
20
40
60
80
100
Time (Days)
-Mel/-Vor
+Mel/-Vor
-Mel/+Vor
+Mel/+Vor
B
GSC267
-Mel/-Vor
–Mel/+Vor
+Mel/-Vor
+Mel/+Vor
H&E

Figure 14. Effect of melatonin and vorinostat treatment on orthotopic xenograft tumor growth and survival.

(A and B) Kaplan-Meier survival curves (A) and representative H&E staining images (B) of mice intracranially injected GSC 267 glioma stem cells. Survival rate significantly increased in the combination treatment group. Tumor margins dramatically inhibited in mice treated with melatonin and vorinostat compared to the control group. Notably, combination treatment decreased tumor volume.

15. Schematic diagram of the mechanism by which vorinostat and melatonin induce TFEB-mediated apoptosis in glioblastoma cells.

We identify the key domain of TFEB mediated tumor survival. Oligomerized TFEB contributes to drug resistance about temozolomide in GBM cell lines. Co-treatment of vorinostat and melatonin inhibits both TFEB expression and TFEB oligomerization. Thereby GBM cell lines were induced apoptosis.

Figure 15

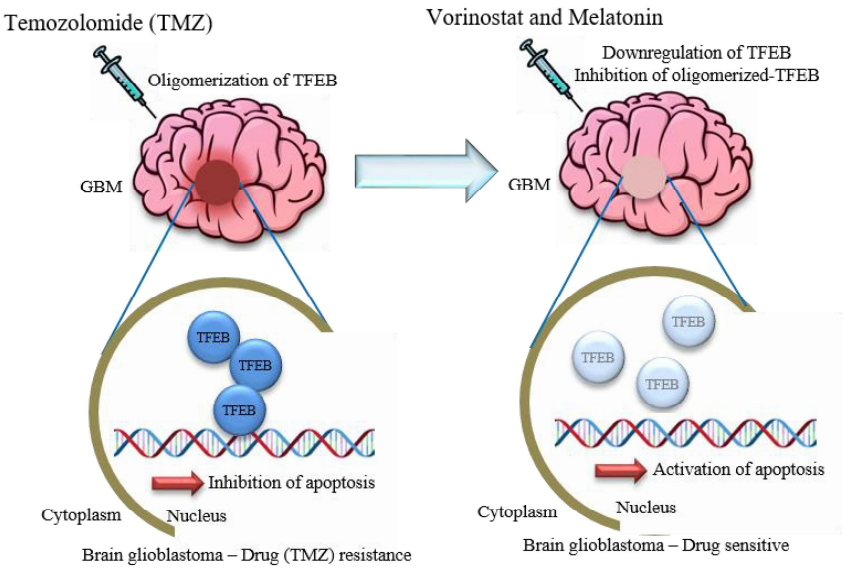
Temozolomide (TMZ)
Oligomerization of TFEB
GBM
TFEB
TFEB
TFEB
Inhibition of apoptosis
Cytoplasm
Nucleus
Brain glioblastoma – Drug (TMZ) resistance
Vorinostat and Melatonin
Downregulation of TFEB
Inhibition of oligomerized-TFEB
GBM
TFEB
TFEB
TFEB
Activation of apoptosis
Cytoplasm
Nucleus
Brain glioblastoma – Drug sensitive

Figure 15. Schematic diagram of the mechanism by which vorinostat and melatonin induce TFEB-mediated apoptosis in glioblastoma cells.

Vorinostat is not sufficient to induce apoptosis of GBM cell lines. With the melatonin, vorinostat promotes therapeutic sensitivity to induce apoptosis in GBM and GSCs.

Discussion

Despite various treatments, including surgical resection, chemotherapy, and radiation therapy, GBM remains an aggressive and incurable brain tumor, with very low 5-year survival rates. Novel therapeutic strategies are therefore needed to treat patients with GBM.

Although TMZ is used to treat patients with GBM and astrocytoma, patients develop resistance to this agent. Combinations of TMZ with other therapeutic agents may overcome TMZ resistance. TMZ-resistant GBM cells are frequently used to investigate drug resistance mechanisms and the efficacy of combination therapy. Efforts have been made to identify target genes that promote GBM tumorigenesis, and patients with GBM have been classified by gene profiling data, allowing the selection of the most effective agents. However, the roles of drug resistance-related target molecules in GBMs remain incompletely understood. We therefore investigated the effect of TFEB, a master regulator of autophagy, on GBM tumorigenesis and drug resistance.

Assessments of the most effective treatments for GBM patients have included studies of TMZ resistance and the regulation of glioma-initiating cell or GSC proliferation. GBMs are a heterogeneous mixture of tumor cells and cancer stem cells, which contribute to tumor initiation and resistance to treatment[45]. GSCs were shown to be more resistant to classical cancer therapy than glioblastoma non-CSCs[46)]. For example, $CD133^{+}$/GSCs showed little response to chemotherapy and radiotherapy. Therefore, treatment of GBMs should include therapeutic strategies targeting GSCs[47-49)]. Our results provide evidence that the combination of vorinostat and melatonin is a novel strategy to inhibit GBM tumorigenesis and the CSC properties of GSCs and GBMs.

Melatonin is a therapeutic agent recently found to reduce cisplatin-induced loss of ovarian follicles by regulating the PI3K signaling pathway[17)]. Although melatonin alone has little effect on GBMs or GSCs, melatonin may upregulate the therapeutic

efficacy of chemotherapy agents. We therefore assessed the ability of melatonin to enhance the efficacy of the HDAC inhibitor vorinostat in GBMs and GSCs.

Vorinostat is a linear hydroxamic acid that inhibits HDAC classes I/II, causing the deacetylation of histones H2A, H2B, H3, and H4 and non-histone proteins[49-51]. Deacetylation of these proteins alters chromatin structure, ultimately altering the transcription activity of target genes. Vorinostat also increases the acetylation state of certain proteins, including p53 and hsp90[52]. Therefore, vorinostat changes the expression of about 10% of disease-related genes and may be effective in a broad range of solid tumors and hematological malignancies. Vorinostat has been reported to affect cells derived from several types of cancer, including head and neck squamous cell carcinoma, CTCL, hepatoma, multiple myeloma, and glioblastoma[53-57].

We found that the combination of vorinostat-melatonin had a synergistic cytotoxic effect in GBM cells through the inhibition of TFEB translocation to and oligomerization in the nucleus, followed by the induction of apoptotic cell death. The combination of vorinostat and melatonin in patients with GBM may have therapeutic efficacy and overcome drug resistance by regulating TFEB expression, translocation, and oligomerization.

TFEB is a master regulator of autophagy and lysosome function, regulating both the expression of lysosomal proteins and lysosomal acidification. TFEB is also involved in diseases such as cancer and inflammatory diseases[58]. TFEB is overexpressed in lung cancers, inducing cell migration and poor prognosis. TFEB overexpression also promotes tumorigenesis, angiogenesis, and metastasis by increasing lysosomal enzyme activity and the secretion of hydrolases into the extracellular space. By contrast, TFEB depletion reduces the migration of cancer cells[59]. We showed that co-treatment with vorinostat and melatonin reduced both nuclear localization and oligomerization of TFEB, thereby inhibiting GBM tumorigenesis and tumor-sphere formation by GSCs.

TFEB binds to gene promoters, regulating the expression of lysosomal genes and of target genes involved in apoptosis and tumorigenesis. Moreover, the interplay of TFEB with various transcription factors and histone modulators results in the

epigenetic regulation of target genes in GBM cells. These findings strongly suggest that GBM cell apoptosis is mediated by the direct association between TFEB expression and the activation of specific epigenetic modulators such as HDACs[58].

Conclusion

In conclusion, our results demonstrate a novel therapeutic strategy and regulatory mechanisms in GBMs. The combination of vorinostat and melatonin induces apoptosis signaling by promoting the oligomerization of TFEB proteins in GBMs. Moreover, co-treatment with vorinostat and melatonin inhibited CSC properties and the proliferation of GSCs by downregulating TFEB expression. This study also provides clinical evidence that the expression of TFEB is critical for GBM tumorigenesis, and that the aggressiveness of human GBM is dependent on TFEB expression. Therefore, the expression and oligomerization of TFEB may be an available therapeutic target for human GBMs and GSCs.

Reference

1. Davis ME. Glioblastoma: Overview of Disease and Treatment. *Clin J Oncol Nurs.* 2016;20(5):S2-8.
2. Becker KP, Baehring JM. Current Standard Treatment Options for Malignant Glioma. In: *Malignant Brain Tumors.*2017:123-131.
3. Ghose A, Lim G, Husain S. Treatment for glioblastoma multiforme: current guidelines and Canadian practice. *Curr Oncol.* 2010;17(6):52-58.
4. Nagarajan RP, Costello JF. Epigenetic mechanisms in glioblastoma multiforme. *Semin Cancer Biol.* 2009;19(3):188-197.
5. Clarke J, Penas C, Pastori C, et al. Epigenetic pathways and glioblastoma treatment. *Epigenetics.* 2013;8(8):785-795.
6. Lee DH, Ryu HW, Won HR, Kwon SH. Advances in epigenetic glioblastoma therapy. *Oncotarget.* 2017;8(11):18577-18589.
7. Gursoy-Yuzugullu O, Carman C, Serafim RB, Myronakis M, Valente V, Price BD. Epigenetic therapy with inhibitors of histone methylation suppresses DNA damage signaling and increases glioma cell radiosensitivity. *Oncotarget.* 2017;8(15):24518-24532.
8. Jung KH, Hong SW, Zheng HM, et al. Melatonin ameliorates cerulein-induced pancreatitis by the modulation of nuclear erythroid 2-related factor 2 and nuclear factor-kappaB in rats. *J Pineal Res.* 2010;48(3):239-250.
9. Reiter RJ, Mayo JC, Tan DX, Sainz RM, Alatorre-Jimenez M, Qin L. Melatonin as an antioxidant: under promises but over delivers. *J Pineal Res.* 2016;61(3):253-278.
10. Pariente R, Pariente JA, Rodriguez AB, Espino J. Melatonin sensitizes human cervical cancer HeLa cells to cisplatin-induced cytotoxicity and apoptosis: effects on oxidative stress and DNA fragmentation. *J Pineal Res.* 2016;60(1):55-64.
11. Park SY, Jang WJ, Yi EY, et al. Melatonin suppresses tumor angiogenesis by inhibiting HIF-1alpha stabilization under hypoxia. *J Pineal Res.*

2010;48(2):178-184.

12. Manchester LC, Coto-Montes A, Boga JA, et al. Melatonin: an ancient molecule that makes oxygen metabolically tolerable. *J Pineal Res.* 2015;59(4):403-419.
13. Tan DX, Manchester LC, Reiter RJ, et al. A novel melatonin metabolite, cyclic 3-hydroxymelatonin: a biomarker of in vivo hydroxyl radical generation. *Biochem Biophys Res Commun.* 1998;253(3):614-620.
14. Reiter RJ, Rosales-Corral SA, Manchester LC, Tan DX. Peripheral reproductive organ health and melatonin: ready for prime time. *Int J Mol Sci.* 2013;14(4):7231-7272.
15. Shiu SY, Pang B, Tam CW, Yao KM. Signal transduction of receptor-mediated antiproliferative action of melatonin on human prostate epithelial cells involves dual activation of Galpha(s) and Galpha(q) proteins. *J Pineal Res.* 2010;49(3):301-311.
16. Casado-Zapico S, Rodriguez-Blanco J, Garcia-Santos G, et al. Synergistic antitumor effect of melatonin with several chemotherapeutic drugs on human Ewing sarcoma cancer cells: potentiation of the extrinsic apoptotic pathway. *J Pineal Res.* 2010;48(1):72-80.
17. Jang H, Na Y, Hong K, et al. Synergistic effect of melatonin and ghrelin in preventing cisplatin-induced ovarian damage via regulation of FOXO3a phosphorylation and binding to the p27(Kip1) promoter in primordial follicles. *J Pineal Res.* 2017;63(3).
18. Reiter RJ, Tan DX, Rosales-Corral S, Manchester LC. The universal nature, unequal distribution and antioxidant functions of melatonin and its derivatives. *Mini Rev Med Chem.* 2013;13(3):373-384.
19. Fan C, Pan Y, Yang Y, et al. HDAC1 inhibition by melatonin leads to suppression of lung adenocarcinoma cells via induction of oxidative stress and activation of apoptotic pathways. *J Pineal Res.* 2015;59(3):321-333.
20. Martina JA, Chen Y, Gucek M, Puertollano R. MTORC1 functions as a transcriptional regulator of autophagy by preventing nuclear transport of

TFEB. *Autophagy.* 2012;8(6):903-914.

21. Song W, Wang F, Savini M, et al. TFEB regulates lysosomal proteostasis. *Hum Mol Genet.* 2013;22(10):1994-2009.

22. Roczniak-Ferguson A, Petit CS, Froehlich F, et al. The transcription factor TFEB links mTORC1 signaling to transcriptional control of lysosome homeostasis. *Sci Signal.* 2012;5(228):ra42.

23. Fang LM, Li B, Guan JJ, et al. Transcription factor EB is involved in autophagy-mediated chemoresistance to doxorubicin in human cancer cells. *Acta Pharmacol Sin.* 2017;38(9):1305-1316.

24. Kim YR, Park MS, Eum KH, et al. Transcriptome analysis indicates TFEB1 and YEATS4 as regulatory transcription factors for drug resistance of ovarian cancer. *Oncotarget.* 2015;6(31):31030-31038.

25. Giatromanolaki A, Sivridis E, Mitrakas A, et al. Autophagy and lysosomal related protein expression patterns in human glioblastoma. *Cancer Biol Ther.* 2014;15(11):1468-1478.

26. Giatromanolaki A, Kalamida D, Sivridis E, et al. Increased expression of transcription factor EB (TFEB) is associated with autophagy, migratory phenotype and poor prognosis in non-small cell lung cancer. *Lung Cancer.* 2015;90(1):98-105.

27. Kauffman EC, Ricketts CJ, Rais-Bahrami S, et al. Molecular genetics and cellular features of TFE3 and TFEB fusion kidney cancers. *Nat Rev Urol.* 2014;11(8):465-475.

28. Clevers H. The cancer stem cell: premises, promises and challenges. *Nat Med.* 2011;17(3):313-319.

29. Altaner C. Glioblastoma and stem cells. *Neoplasma.* 2008;55(5):369-374.

30. Gilbertson RJ, Rich JN. Making a tumour's bed: glioblastoma stem cells and the vascular niche. *Nat Rev Cancer.* 2007;7(10):733-736.

31. Auffinger B, Spencer D, Pytel P, Ahmed AU, Lesniak MS. The role of glioma stem cells in chemotherapy resistance and glioblastoma multiforme recurrence. *Expert Rev Neurother.* 2015;15(7):741-752.

32. Zhang Y, Liu Q, Wang F, et al. Melatonin antagonizes hypoxia-mediated glioblastoma cell migration and invasion via inhibition of HIF-1alpha. *J Pineal Res.* 2013;55(2):121-130.

33. Chen X, Hao A, Li X, et al. Melatonin inhibits tumorigenicity of glioblastoma stem-like cells via the AKT-EZH2-STAT3 signaling axis. *J Pineal Res.* 2016;61(2):208-217.

34. Yamanishi M, Narazaki H, Asano T. Melatonin overcomes resistance to clofarabine in two leukemic cell lines by increased expression of deoxycytidine kinase. *Exp Hematol.* 2015;43(3):207-214.

35. Martin V, Sanchez-Sanchez AM, Herrera F, et al. Melatonin-induced methylation of the ABCG2/BCRP promoter as a novel mechanism to overcome multidrug resistance in brain tumour stem cells. *Br J Cancer.* 2013;108(10):2005-2012.

36. Rhodes DR, Kalyana-Sundaram S, Mahavisno V, et al. Oncomine 3.0: genes, pathways, and networks in a collection of 18,000 cancer gene expression profiles. *Neoplasia.* 2007;9(2):166-180.

37. Santaguida S, Vasile E, White E, Amon A. Aneuploidy-induced cellular stresses limit autophagic degradation. *Genes Dev.* 2015;29(19):2010-2021.

38. Sherr CJ, Roberts JM. CDK inhibitors: positive and negative regulators of G1-phase progression. *Genes Dev.* 1999;13(12):1501-1512.

39. Dijkers PF, Medema RH, Pals C, et al. Forkhead transcription factor FKHR-L1 modulates cytokine-dependent transcriptional regulation of p27(KIP1). *Mol Cell Biol.* 2000;20(24):9138-9148.

40. Zhao H, Wu QQ, Cao LF, et al. Melatonin inhibits endoplasmic reticulum stress and epithelial-mesenchymal transition during bleomycin-induced pulmonary fibrosis in mice. *PLoS One.* 2014;9(5):e97266.

41. Parlakpinar H, Sahna E, Ozer MK, Ozugurlu F, Vardi N, Acet A. Physiological and pharmacological concentrations of melatonin protect against cisplatin-induced acute renal injury. *J Pineal Res.* 2002;33(3):161-166.

42. Nakano I, Hemmati HD, Kornblum HI. [Cancer stem cells in pediatric brain

tumors]. *No Shinkei Geka.* 2004;32(8):827-834.

43. Singh SK, Clarke ID, Terasaki M, et al. Identification of a cancer stem cell in human brain tumors. *Cancer Res.* 2003;63(18):5821-5828.

44. Singh SK, Hawkins C, Clarke ID, et al. Identification of human brain tumour initiating cells. *Nature.* 2004;432(7015):396-401.

45. Kim SH, Ezhilarasan R, Phillips E, et al. Serine/Threonine Kinase MLK4 Determines Mesenchymal Identity in Glioma Stem Cells in an NF-kappaB-dependent Manner. *Cancer Cell.* 2016;29(2):201-213.

46. Choi J, Lee JH, Koh I, et al. Inhibiting stemness and invasive properties of glioblastoma tumorsphere by combined treatment with temozolomide and a newly designed biguanide (HL156A). *Oncotarget.* 2016;7(40):65643-65659.

47. Vescovi AL, Galli R, Reynolds BA. Brain tumour stem cells. *Nat Rev Cancer.* 2006;6(6):425-436.

48. Beier D, Schulz JB, Beier CP. Chemoresistance of glioblastoma cancer stem cells--much more complex than expected. *Mol Cancer.* 2011;10:128.

49. Bao S, Wu Q, McLendon RE, et al. Glioma stem cells promote radioresistance by preferential activation of the DNA damage response. *Nature.* 2006;444(7120):756-760.

50. Liu G, Yuan X, Zeng Z, et al. Analysis of gene expression and chemoresistance of CD133+ cancer stem cells in glioblastoma. *Mol Cancer.* 2006;5:67.

51. Kim EH, Lee JH, Oh Y, et al. Inhibition of glioblastoma tumorspheres by combined treatment with 2-deoxyglucose and metformin. *Neuro Oncol.* 2017;19(2):197-207.

52. Sundar SJ, Hsieh JK, Manjila S, Lathia JD, Sloan A. The role of cancer stem cells in glioblastoma. *Neurosurg Focus.* 2014;37(6):E6.

53. Zhu Z, Jiang W, McGinley JN, Thompson HJ. 2-Deoxyglucose as an energy restriction mimetic agent: effects on mammary carcinogenesis and on mammary tumor cell growth in vitro. *Cancer Res.* 2005;65(15):7023-7030.

54. Owen MR, Halestrap AP. The mechanisms by which mild respiratory chain

inhibitors inhibit hepatic gluconeogenesis. *Biochim Biophys Acta.* 1993;1142(1-2):11-22.

55. Wallace DC. Mitochondria and cancer. *Nat Rev Cancer.* 2012;12(10):685-698.

56. Kang SG, Cheong JH, Huh YM, Kim EH, Kim SH, Chang JH. Potential use of glioblastoma tumorsphere: clinical credentialing. *Arch Pharm Res.* 2015;38(3):402-407.

57. Gatenby RA, Gillies RJ. Why do cancers have high aerobic glycolysis? *Nat Rev Cancer.* 2004;4(11):891-899.

58. Brady OA, Martina JA, Puertollano R. Emerging roles for TFEB in the immune response and inflammation. *Autophagy.* 2017:1-9.

59. Magini A, Polchi A, Di Meo D, et al. TFEB activation restores migration ability to Tsc1-deficient adult neural stem/progenitor cells. *Hum Mol Genet.* 2017;26(17):3303-3312

국문 요약

교모세포종은 가장 공격적이며 가장 치명적인 뇌종양의 형태입니다. 또한 수많은 암중에서도 가장 치료비가 비싼 종류이며 수술, 방사선 치료, 항암치료를 통한 처치역시 힘든 암입니다. Oncomine platform analysis와 Gene Expression Profiling Interactive Analysis (GEPIA)에 따르면 4기 교모세포종 환자들에게서 TFEB 단백질이 확연하게 증가합니다. TFEB는 전사인자로써 기능하기 위하여 중합체 형성과 핵으로의 이동을 필요로 합니다. TFEB 단백질의 발현과 중합체형성은 교모세포종의 TMZ와 같은 전통적인 약물에 대한 저항성에 기여합니다. 그래서 교모세포종과 뇌종양줄기세포에서 멜라토닌과 보리노스탯의 병용 투여를 통해 TFEB의 효과를 극복하고 세포예정사를 유도하고자 하였습니다. 보리노스탯과 멜라토닌에 의해 TFEB의 발현과 중합체 형성이 억제되자 세포예정사 연관 단백질들의 발현양이 증가하였으며 세포예정사가 활성화 되었습니다. 특히 TFEB의 발현을 억제하자 뇌종양줄기세포의 종양구 형성과 크기가 확연하게 감소하였습니다. 병용투여의 결과 뇌종양줄기세포의 증식이 감소하였을 뿐만 아니라 cleaved-PARP와 p-γH2AX를 유도하였습니다. 정리하자면, TFEB 발현은 교모세포종의 항암제저항성 형성에 기여하며 보리노스탯과 멜라토닌의 병용투여를 통해 TFEB의 발현과 중합체형성을 억제함으로써 교모세포종의 사멸을 유도할 수 있습니다. 그러므로 보리노스탯과 멜라토닌은 교모세포종의 치료에 있어서 효율적인 치료 전략으로 사용 될 수 있습니다.

중심단어: TFEB, 중합체 형성, 분포, 교모세포종, 뇌종양줄기세포, 항암제저항성

Acknowledgement

오랫동안 준비해온 학위 논문을 마무리 하게 되었습니다. 처음 2014년에 석사 학위에 입학하여 2019년에 박사학위를 마무리 하게 되기까지 정말 많은 분들을 만나고 도움을 받아서 여기까지 올 수 있었던 것 같습니다. 그 중에서도 지도교수님이신 최경철 교수님께 가장 큰 감사의 말씀을 드립니다. 항상 저의 실험에 관심을 기울여 주시고 올바른 방향으로 향할 수 있도록 지도해주셨기에 좋은 결과를 얻을 수 있었다고 생각합니다. 진심으로 감사드리며 도움이 되는 제자가 될 수 있도록 노력하겠습니다. 또한 많이 부족한 학위 논문을 지도해 주시고 심사해 주신 손재경 교수님, 하창훈 교수님, 신용 교수님, 김성학 교수님께 진심으로 감사드립니다. 그리고 저희 교실에서 많은 조언과 관심을 보내주신 신동명 교수님과 김승후 교수님, 장은주 교수님께도 감사의 말씀을 드립니다.

석사과정에서부터 지금에 이르기까지 긴 과정동안 많은 분들의 도움을 받아왔다고 생각합니다. 먼저 저에게 처음으로 실험을 가르쳐주고 기초를 알려주신 영신이형과 미현누나에게 감사드리며 저희 실험실에서 박사과정 내내 함께 실험한 동료들인 곽성민, 송지혜, 박승호, 정지훈, 김현희에게도 감사의 인사를 전합니다. 모두 좋은 논문과 함께 보람찬 학위과정을 보낼 수 있을 것이라고 믿으며 함께 학위과정을 할 수 있어서 영광이였습니다. 그리고 지도교수님이신 최경철 교수님의 지도교수님이시며 첫 해외학회를 참석하는데 도와주시고 큰 경험을 할 수 있게 도와주신 윤호근 교수님과 최효경 박사님, 박수연 박사님, 서재성 박사님, 이승현 박사님께도 감사드립니다.

또 같이 학위과정을 진행하며 많은 도움을 받은 손재경 교수님 실험실의 김지혜, 조영라, 이지현, 김종욱에게도 감사드립니다. 특히 박사과정 동기인 김지혜에게 감사드립니다. 참여가 강제되지 않는 저널미팅에까지 참여하여 연구에 대한 열정을 불태우는 모습을 보며 느슨해지는 자신을 다잡게 되었습니다. 그리고 학위과정을 진행한다고 연락도 잘 안하고 자주 볼 수도 없었음에도 언제나 반갑게 대해주고 항상 응원해주던 제 친구들 근석, 정현, 의선, 성웅, 승현, 태웅, 준철에게도 감사드립니다. 표현을 자주 안 해서 미안하지만 항상 고맙게 생각합니다.

마지막으로 소중한 저의 가족들에게 감사의 말씀을 드립니다. 언제나 마음속에 든든한 벽이 되어 지켜주신 아버지와 나가 살고 있는 아들을 항상 걱정하시

며 좋은 것들을 볼 때마다 아들 생각하셔서 계속 보내주신 어머니, 이제는 자리를 잡고 부모님을 잘 챙겨주는 누나까지 모두 감사드립니다. 그리고 학위과정 중에 결혼하게 되어 믿음직스럽지 못하였을 텐데도 항상 믿고 응원해주신 장인어른과 장모님에게도 감사드립니다. 앞으로 그 믿음에 보답할 수 있도록 노력하겠습니다. 소중하고 소중한 부인 신재희에게 진심으로 감사드립니다. 학위과정을 한다고 집에도 늦게 들어오고 또래 친구들처럼 자유롭게 보낼 수 없었을 텐데도 항상 응원해준 그 마음에 진심으로 감사하고 남은 삶 동안 꼭 갚아나가겠습니다.

2019년 6월 24일 논문을 마무리하며 감사의 마음을 전합니다.

성기준